AD_____

Award Number: DAMD17-02-1-0171

TITLE: Role of Oligomeric α-Synuclein in Mitochondrial Membrane Permeabilization and Neurodegeneration in Parkinson's Disease

PRINCIPAL INVESTIGATOR: Seung-Jae Lee, Ph.D.

CONTRACTING ORGANIZATION: The Parkinson's Institute
Sunnyvale, California 94089-1605

REPORT DATE: December 2002

TYPE OF REPORT: Annual

PREPARED FOR: U.S. Army Medical Research and Materiel Command
Fort Detrick, Maryland 21702-5012

REPORT DOCUMENTATION PAGE

Form Approved
OMB No. 074-0188

1. AGENCY USE ONLY (Leave blank)	2. REPORT DATE	3. REPORT TYPE AND DATES COVERED
	December 2002	Annual (19 Nov 01 - 18 Nov 02)

4. TITLE AND SUBTITLE
Role of Oligomeric α-Synuclein in Mitochondrial Membrane Permeabilization and Neurodegeneration in Parkinson's Disease

5. FUNDING NUMBERS
DAMD17-02-1-0171

6. AUTHOR(S) :
Seung-Jae Lee, Ph.D.

7. PERFORMING ORGANIZATION NAME(S) AND ADDRESS(ES)
The Parkinson's Institute
Sunnyvale, California 94089-1605

E-Mail: Slee@thepi.org

8. PERFORMING ORGANIZATION REPORT NUMBER

9. SPONSORING / MONITORING AGENCY NAME(S) AND ADDRESS(ES)
U.S. Army Medical Research and Materiel Command
Fort Detrick, Maryland 21702-5012

10. SPONSORING / MONITORING AGENCY REPORT NUMBER

11. SUPPLEMENTARY NOTES
report contains color

12a. DISTRIBUTION / AVAILABILITY STATEMENT
Approved for Public Release; Distribution Unlimited

12b. DISTRIBUTION CODE

13. Abstract ***(Maximum 200 Words)*** *(abstract should contain no proprietary or confidential information)*

Amyloid-like fibrillar aggregate of α-synuclein is a common pathological feature of many neurological disorders, including Parkinson's disease. Interestingly, in vitro studies revealed various non-fibrillar intermediate species during the course of fibrillation, raising a question as to which of these aggregates are pathogenic species. The goal of the current project is to identify and characterize the cellular α-synuclein aggregates and to assess the effects of these aggregates. We have established a biochemical fractionation method to separate α-synuclein aggregate subspecies from the cytoplasm. Characterization of these subspecies, using electron microscopy and confocal microscopy, showed that cellular fibrillation also involves non-fibrillar intermediates and that these intermediates need to be accumulated in the pericentriolar region by a microtubule-dependent mechanism in order to form fibrils. We also found that the formation of non-fibrillar intermediates was tightly associated with the fragmentation of the Golgi apparatus, whereas the formation of fibril-rich inclusion bodies occurred after the Golgi fragmentation. Our study suggests that the prefibrillar intermediates can cause impairment of specific cytoplasmic organelles, and we are currently investigating cytotoxic effects of these aggregates in both non-neuronal and neuronal cell types.

14. SUBJECT TERMS
Parkinson's Disease, synuclein, fibril, protein aggregate, Golgi apparatus, inclusion body, microtubule

15. NUMBER OF PAGES
95

16. PRICE CODE

17. SECURITY CLASSIFICATION OF REPORT	18. SECURITY CLASSIFICATION OF THIS PAGE	19. SECURITY CLASSIFICATION OF ABSTRACT	20. LIMITATION OF ABSTRACT
Unclassified	Unclassified	Unclassified	Unlimited

Table of Contents

A. Introduction

Many human neurological disorders, including Parkinson's disease, dementia with Lewy bodies, and multiple system atrophy, are characterized by amyloid-like fibrillar aggregates of α-synuclein, such as Lewy bodies (LBs) and Lewy neurites (Hardy and Gwinn-Hardy, 1998; Trojanowski et al., 1998). While the direct role of fibrils and inclusion bodies in disease progression is the subject of intense debate, recent *in vitro* studies revealed various non-fibrillar species during the course of fibrillation and suggested a possibility that these metastable intermediate species, not the fibrils themselves, might elicit cytotoxicity (Conway et al., 2000; Conway et al., 2001). Elucidating which particular aggregate species possess the principal cytotoxic effect holds the key to understanding the etiologic role of protein aggregation in the disease pathogenesis. Study of this problem, however, has been hampered by the lack of experimental system in which intermediates of the endogenous fibrillation process can be biochemically defined and analyzed. We have recently established such an experimental cell system, and the goal of the current study is to elucidate the mechanisms of α-synuclein fibrillation and assess the effects of prefibrillar intermediates in the cytoplasm.

B. Body (The revised Statement of Work, which was submitted earlier, is attached as appendix 3)

B.1. Mechanisms of α-synuclein fibrillation and inclusion formation in cells

In order to understand the mechanism of α-synuclein aggregation in cells, the first objective of our study was to characterize the structural and compositional properties of different aggregate species. Specifically, we have addressed following questions. (i) What is the end product of α-synuclein aggregation process in cells? (i.e., is it the fibril or other aggregate form?) (ii) What are the intermediates of α-synuclein fibrillation in cells? (iii) Is the fibrillation process linked to the inclusion formation process and if so, how? In this study, using a combination of biochemical fractionation, immunofluorescence labeling, and electron microscopy (EM), we have accomplished following. For details, see appendix (A) 1, Lee and Lee. Figures that are referenced in this section can be found in A1.

1. ***Isolation of different aggregate species from the cytoplasm.*** Overexpression of α-synuclein in cells spontaneously produce two types of aggregates that are distinct in their sizes and cytoplasmic distributions. One type is represented by small punctate aggregates that are dispersed throughout the cytoplasm, and the other is large juxtanuclear inclusion bodies (Fig 1). In order to further characterize different types of α-synuclein aggregates, these aggregates were separated using a series of extractions and differential and density-gradient centrifugations (for details, see Fig. 2A and materials and methods in appendix 1). Western blot analysis of the fractions (frs) has identified three distinct fractions containing SDS-resistant α-synuclein aggregates (fr 2, fr 4, and 80 g pellet) (Fig. 2B), confirming the presence of different aggregate species.

2. ***Structural properties of cytoplasmic aggregates.*** The juxtanuclear inclusion bodies bind to thioflavin S (Fig. 1B and 3), a fluorescent dye specific for the highly ordered cross β-sheet structure, thus an indicative of the amyloid-like fibrillar structures. In contrast, the small punctate aggregates (both the frs 2 and 4) are thioflavin S-negative (Fig. 1A and 3),

indicating a non-fibrillar conformation. The difference in the dye binding properties suggests that these two types of aggregates have different structural properties. To further analyze the ultrastructural features of α-synuclein aggregates, the fractions were examined by immuno-EM. The aggregates in both the fr 2 and fr 4 appear to be non-fibrillar spheres (Fig. 4A and B). Random measurement of the diameter of these spheres shows the different size distributions, and the calculated mean diameters for fr 2 and fr 4 were 24 nm and 34 nm, respectively. On the other hand, EM analysis showed that the 80 g pellet contained the large inclusion bodies that are filled with fibril structures (Fig. 5A and B). The fibrils isolated from the inclusions are 8-13 nm in width and are clearly labeled with α-synuclein antibody (Fig. 5B). These fibrils resemble the ones isolated from human LBs (Spillantini et al., 1998) or the inclusions of the transgenic mice (Giasson et al., 2002). Thicker structures, which appear to be fibril bundles, are also frequently observed (Fig. 5C). These ultrastructural morphologies, along with the thioflavin S binding property, demonstrate that α-synuclein aggregation process in our cell model produces the inclusion bodies that are composed of α-synuclein fibrils, thus suggesting that this process of inclusion body formation in these cells may resemble the process of LB formation in human brain.

3. ***Compositional properties of cytoplasmic aggregates.*** To determine whether the inclusion bodies in our cell system share the protein components with human LBs, we co-stained the cells for α-synuclein with ubiquitin, α-subunit of 20S proteasome, or hsp70 (Auluck et al., 2002; Ii et al., 1997; Spillantini et al., 1998). Like human LBs, large juxtanuclear inclusion bodies were positive for all these proteins (Fig. 1 B). On the other hand, most of peripheral punctate aggregates were not stained with ubiquitin, the proteasome subunit, or hsp70 (Fig. 1A). Consistent with these findings, immunofluorescence staining of the fractionated aggregates showed that the small aggregates did not contain ubiquitin, hsp70, or 20S proteasome α-subunit, whereas the large inclusion bodies in the 80 g pellet were positive for these proteins (Fig. 3B, C, and D). These results confirm that the cells produce different types of α-synuclein aggregates with distinct conformational and compositional properties and that the separation of these aggregates can be achieved using our fractionation procedure.

4. ***Protofibril-to-fibril transition in the cytoplasm is linked to the microtubule-dependent inclusion-forming process.*** Time course analysis of the aggregates showed that the fr 2 aggregates appeared first, followed by the fr 4 aggregates and subsequently by the fibrillar inclusion bodies (Fig. 6). The fact that these aggregates appear sequentially suggests precursor-product relationship between them. It has been demonstrated with a number of proteins that the juxtanuclear inclusion formation requires the microtubule-dependent transport of peripheral small aggregates to the pericentriolar region (Garcia-Mata et al., 1999; Johnston et al., 1998). To test if microtubule-dependent transport is important for the formation of α-synuclein inclusion body, we treated the cells with a microtubule-disrupting agent, nocodazole, and assessed the inclusion formation in two ways. First, the number of inclusion bodies was counted after the immunofluorescence staining (Fig. 7A). Second, the relative amounts of inclusion bodies and small non-fibrillar aggregates were measured after the fractionation (Fig. 7B). Both analyses clearly show the decrease of the inclusion bodies after nocodazole treatment, implicating the

importance of microtubule-dependent transport system in the inclusion formation. Furthermore, the fractionation experiment shows that the reduction of inclusion bodies is accompanied by the increase of the small aggregates (Fig. 7B), confirming that the small spherical aggregates are the precursors for the fibrillar inclusions. Interestingly, when the microtubule is disrupted, bigger foci were frequently found in the periphery of the cell (Fig. 7C), which implies that the peripheral aggregates can grow bigger to a certain extent, if their transport to the pericentriolar region is blocked. This finding raised a question as to whether the large foci that are grown in the periphery of the cell can acquire the characteristics of the juxtanuclear inclusion bodies. To address this question, we have investigated the thioflavin S binding property and the immunoreactivities for the proteins that are found in the inclusion bodies. Unlike the juxtanuclear inclusion bodies, the large peripheral foci are thioflavin S-negative, indicating non-fibrillar nature of the aggregates, and devoid of ubiquitin, hsp70, and 20S proteasome α-subunit (Fig. 7C). These data suggest that fibrillation and acquisition of the auxiliary proteins are not spontaneous consequences of the aggregate growth, rather they are closely linked to the microtubule-dependent inclusion-forming process.

B.2. Golgi fragmentation in the cells that produce prefibrillar α-synuclein aggregates

As part of the effort to find the pathogenic aggregate species and their cellular targets, we have tested the hypothesis that formation of prefibrillar oligomeric α-synuclein causes Golgi fragmentation. This study was made possible by the establishment of the cell culture model system, in which the effects of monomer and different types of α-synuclein aggregates can be distinguished. The results of the study using this cell system are summarized. For details, see A2, Gosavi et al. Figures that are referenced in this section can be found in A2.

1. ***Association between Golgi fragmentation and the formation of prefibrillar α-synuclein aggregates.*** To investigate cellular consequences specific to α-synuclein aggregation, we have analyzed the morphological integrity of Golgi apparatus (GA) with respect to the α-synuclein aggregation states using an immunofluorescence microscopy with the antibody against a cis-Golgi-specific matrix protein GM130. In cells with diffuse α-synuclein staining, the GA has normal compact morphology near the nucleus (Fig. 3A). However, the cells with prefibrillar aggregates frequently show fragmentation and dispersion of the GA (Fig. 3B and C). Golgi fragmentation was found far more frequently in the population with the aggregates (88.9%) than in general population (11.5%) (Fig. 3E). To further determine if Golgi fragmentation is aggregation-induced event, cells with fragmented Golgi were counted at different α-synuclein expression conditions. Expression of a high-level of soluble α-synuclein did not affect the Golgi fragmentation. On the other hand, the Golgi fragmentation was significantly increased in the condition where prefibrillar aggregates formed with stable monomer levels (Fig. 3D). These results suggest that increase of α-synuclein aggregates, rather than the monomer, might be the cause of Golgi fragmentation.

2. ***Absence of correlation between Golgi fragmentation and fibrillar inclusion body.*** In contrast to the prefibrillar aggregates, no clear association was found between the fibrillar inclusions and the Golgi fragmentation. First, increase in Golgi fragmentation occurs before the appearance of fibrillar inclusions (Fig. 2B and 3F). Secondly, the size of the

cell population that contains fragmented GA does not increase during the period when a sudden increase in the number of fibrillar inclusions takes place (Fig. 2B and 3F). Finally, fragmented GA was rarely observed in the cells with fibrillar inclusions. Instead, two types of GA morphology were associated with fibrillar inclusions: in most cases, Golgi components were confined and dispersed inside the fibrillar inclusions (Fig. 7A), and occasionally, some cells maintained the compact, although slightly distorted, morphology of GA that surrounded the juxtanuclear fibrillar inclusions (Fig. 7B). The fact that Golgi fragmentation occurs before the formation of inclusions and that some cells maintain the compact Golgi structure despite the presence of inclusions suggests that the inclusions themselves may not be the direct cause of the morphological disruption of the GA. Rather, co-staining of the fibrillar inclusions with α-synuclein and Golgi marker suggests that the inclusions might be a consequence of the cell's attempt to remove abnormal protein aggregates and impaired organelles from the cytoplasm.

3. ***Juxtanuclear inclusion bodies may represent cellular response to toxic protein aggregation and impairment of organelles.*** Lysosomes and mitochondria, which normally tend to be dispersed in the cytoplasm, showed a rather localized pattern in the juxtanuclear region in the presence of the prefibrillar α-synuclein aggregates (Fig. 8A and C). These organelles showed no sign of fragmentation and appear to be functionally intact. EM study also showed the accumulation of fragmented Golgi (Fig. 9, box 1) and intact mitochondria in the juxtanuclear region (Fig. 9). In addition, autophagosomes and lysosomes can be found in this area at the early stage of inclusion formation (Fig. 9, box 2). Proteasomes and chaperone molecules were also accumulated near the nucleus in the cells with α-synuclein aggregates. It has been suggested that the juxtanuclear pericentriolar region serves as the main location in which both autophagic-lysosomal system and ubiquitin-proteasome system execute their degradation function to remove abnormal proteins and damaged organelles (Garcia-Mata et al., 2002; Kopito, 2000; Wigley et al., 1999). Thus, the localization of functional lysosomes and mitochondria in the juxtanuclear region may be the manifestation of cell's defense mechanisms against the protein aggregates. Together, these results suggest that the formation of α-synuclein aggregates trigger the action of cellular defense system, which is represented by the accumulation of these aggregates and impaired organelles in the juxtanuclear region along with the mitochondria, autophagosomes/lysosomes, and proteasomes.

C. Key Research Accomplishments

- Biochemical fractionation method to separate the α-synuclein aggregate subspecies from the cytoplasm has been established.

- The fractionation and EM studies show that the juxtanuclear inclusion bodies are filled with α-synuclein fibrils and that at least two different prefibrillar spherical aggregates are formed in the course of fibrillation.

- Time-course and microtubule-disruption experiments show that spherical aggregates are the precursors for fibrillar inclusion bodies.

- α-Synuclein fibrillation in cells is tightly coordinated with the microtubule-dependent inclusion-forming process.

- Formation of prefibrillar oligomeric α-synuclein aggregates is associated with Golgi fragmentation, suggesting the prefibrillar intermediates as being pathogenic species.

- Fibrillar inclusion bodies seem to be a consequence of cellular effort to remove toxic protein aggregates and damaged organelles from cytoplasm.

D. Reportable Outcomes

Publications

Lee H-J, Lee S-J (2002) Characterization of cytoplasmic α-synuclein aggregates: Fibril formation is tightly linked to the inclusion forming process in cells. *J. Biol. Chem.* in press

Gosavi N, Lee H-J, Lee JS, Patel S, Lee S-J (2002) Golgi Fragmentation Occurs in the Cells with prefibrillar α-Synuclein aggregates and Precedes the Formation of Fibrillar Inclusion. *J. Biol. Chem.* in press

Manuscript submitted

Lee S-J (2002) α-Synuclein aggregation: a link between mitochondrial defects and Parkinson's disease? (Review) *Submitted to Antiox. Redox Signal.*

Presentations

Lee S-J (Jun. 2002) Golgi fragmentation and reduced cell viability in cells with prefibrillar α-synuclein aggregates. *FASEB Summer Conference on "Amyloids and Other Abnormal Protein Folding Processes"* Snowmass Village, CO

Lee H-J, Lee S-J (Jun. 2002) Isolation and characterization of α-synuclein aggregates in cells exposed to mitochondrial inhibitors. *FASEB Summer Conference on "Amyloids and Other Abnormal Protein Folding Processes"* Snowmass Village, CO

Lee H-J, Lee S-J (Nov. 2002) Isolation and characterization of aggregates from cells that overexpress α-synuclein. *Society for Neuroscience 32nd annual meeting*, Orlando, FL

Gosavi N, Lee H-J, Lee JS, Patel S, Lee S-J (Nov. 2002) Golgi fragmentation and reduced cell viability by prefibrillar α-synuclein aggregates. *Society for Neuroscience 32nd annual meeting*, Orlando, FL

Funding applied for based on work supported by this award

2002-2004 Michael J. Fox Foundation for Parkinson's Research (Awarded)

Title: Role of autophagic-lysosomal pathway in the degradation of α-synuclein aggregates (This project is to study the mechanism of the aggregate breakdown in cells, and characteristics of α-synuclein aggregates discovered in the current study enabled us to propose the study by which specific target aggregates of the degradation pathway will be identified.)

2003-2005 Michael J. Fox Foundation for Parkinson's Research (Pending)
Title: Study of the metabolism and aggregation of α-synuclein in parkin-depleted neuronal cells (The fractionation of α-synuclein aggregates is a key component of this proposal.)

E. Conclusions

LBs, α-synuclein inclusions in brain, contain fibrillar aggregates of α-synuclein, implying that the fibrillation process *in vivo* is somehow integrated into the inclusion-forming process. In an attempt to understand α-synuclein fibrillation in the context of inclusion-forming process, our group established a cell system in which overexpression of α-synuclein resulted in inclusion bodies. In these cells, small punctate aggregates appeared at early time points throughout the cytoplasm, followed by large pericentriolar inclusion bodies. Using ultrastructural characterization and fibril-specific dye-binding analysis, we have demonstrated that the small aggregates are non-fibrillar spherical aggregates and the inclusion bodies are filled with fibrillar aggregates that resemble the ones found in the LBs. These results suggest that *in vivo,* α-synuclein fibrillation utilizes the same principle as the *in vitro* process such that protofibrillar intermediates are involved in the fibrillation. In addition, we obtained the evidence that in cells, the protofibril-to-fibril transition is not a diffusion-driven process and requires microtubule-dependent deposition of protofibrils in the pericentriolar region. This study clearly demonstrates that *in vivo,* α-synuclein fibrillation is tightly linked to the microtubule-dependent inclusion-forming process.

Establishment and characterization of our cell culture model enabled us to discover that α-synuclein aggregation was associated with fragmentation of Golgi apparatus and impairment of protein trafficking through the biosynthetic pathway. Although it is not clear as yet whether Golgi fragmentation is linked to cell death, these results support the notion that α-synuclein gains pathogenic function through forming higher order quaternary structures to damage specific cellular targets. Interestingly, the same study showed that Golgi fragmentation was tightly correlated with the production of prefibrillar aggregates, but not with the formation of fibrillar inclusions, suggesting that the prefibrillar aggregates might be responsible for the cellular impairments.

Having established a cell culture system that produces both protofibrils and fibrillar inclusions, we are now in a position to pursue two of the most critical questions in neurodegeneration research. These are *(1) What is the nature of the pathogenic protein aggregates and (2) What are the specific targets of these aggregates that are relevant to the degeneration mechanisms*. The studies we are currently undertaking will provide specific link between α-synuclein aggregation and cellular impairment, and could very well lead to the identification of the specific aggregate species that are relevant to the pathogenesis of the α-synucleinopathies. These studies could also shed light on the longstanding debate as to whether or not Lewy bodies are harmful or protective. Finally, answering these essential questions could open up an entirely new therapeutic approach to the Lewy body diseases, such as Parkinson's disease, which could lead to strategies to slow or halt disease progression.

We are currently investigating the effects of α-synuclein aggregation and Golgi fragmentation on cell viability, which was proposed in the Statement of Work. In addition, having obtained critical mass of knowledge on the aggregation behavior of α-synuclein in mammalian cell system, we recommend confirming our findings in a dopamine-producing neuronal cell system, which is more relevant to PD than our current cell system.

F. References

Auluck, P.K., H.Y. Chan, J.Q. Trojanowski, V.M. Lee, and N.M. Bonini. 2002. Chaperone suppression of alpha-synuclein toxicity in a Drosophila model for Parkinson's disease. *Science*. 295:865-8.

Conway, K.A., S.-J. Lee, J.C. Rochet, T.T. Ding, R.E. Williamson, and P.T. Lansbury, Jr. 2000. Acceleration of oligomerization, not fibrillization, is a shared property of both alpha-synuclein mutations linked to early-onset Parkinson's disease: implications for pathogenesis and therapy. *Proc Natl Acad Sci U S A*. 97:571-6.

Conway, K.A., J.C. Rochet, R.M. Bieganski, and P.T. Lansbury, Jr. 2001. Kinetic stabilization of the alpha-synuclein protofibril by a dopamine- alpha-synuclein adduct. *Science*. 294:1346-9.

Garcia-Mata, R., Z. Bebok, E.J. Sorscher, and E.S. Sztul. 1999. Characterization and dynamics of aggresome formation by a cytosolic GFP- chimera. *J Cell Biol*. 146:1239-54.

Garcia-Mata, R., Y.S. Gao, and E. Sztul. 2002. Hassles with Taking Out the Garbage: Aggravating Aggresomes. *Traffic*. 3:388-396.

Giasson, B.I., J.E. Duda, S.M. Quinn, B. Zhang, J.Q. Trojanowski, and V.M.-Y. Lee. 2002. Neuronal alpha-Synucleinopathy with Severe Movement Disorder in Mice Expressing A53T Human alpha-Synuclein. *Neuron*. 34:521-533.

Hardy, J., and K. Gwinn-Hardy. 1998. Genetic classification of primary neurodegenerative disease. *Science*. 282:1075-9.

Ii, K., H. Ito, K. Tanaka, and A. Hirano. 1997. Immunocytochemical co-localization of the proteasome in ubiquitinated structures in neurodegenerative diseases and the elderly. *J Neuropathol Exp Neurol*. 56:125-31.

Johnston, J.A., C.L. Ward, and R.R. Kopito. 1998. Aggresomes: a cellular response to misfolded proteins. *J Cell Biol*. 143:1883-98.

Kopito, R.R. 2000. Aggresomes, inclusion bodies and protein aggregation. *Trends Cell Biol*. 10:524-30.

Spillantini, M.G., R.A. Crowther, R. Jakes, M. Hasegawa, and M. Goedert. 1998. alpha-Synuclein in filamentous inclusions of Lewy bodies from Parkinson's disease and dementia with lewy bodies. *Proc Natl Acad Sci U S A*. 95:6469-73.

Trojanowski, J.Q., M. Goedert, T. Iwatsubo, and V.M. Lee. 1998. Fatal attractions: abnormal protein aggregation and neuron death in Parkinson's disease and Lewy body dementia. *Cell Death Differ*. 5:832-7.

Wigley, W.C., R.P. Fabunmi, M.G. Lee, C.R. Marino, S. Muallem, G.N. DeMartino, and P.J. Thomas. 1999. Dynamic association of proteasomal machinery with the centrosome. *J Cell Biol*. 145:481-90.

Appendix 1

Characterization of cytoplasmic α-synuclein aggregates: Fibril formation is tightly linked to the inclusion forming process in cells

He-Jin Lee and Seung-Jae Lee*

The Parkinson's Institute, Sunnyvale, CA 94089

*All Correspondence should be addressed to Seung-Jae Lee: The Parkinson's Institute, 1170 Morse Avenue, Sunnyvale, CA 94089, Tel: 408-542-5642, Fax: 408-734-8522, Email: slee@thepi.org

Running title: α-synuclein fibrillation in cells

This work was supported by the U. S. Army Medical Research Acquisition Activity (DAMD17-02-0171) and the Abramson Family Foundation.

Summary

α-Synuclein fibrillation process has been associated with the pathogenesis of several neurodegenerative diseases. Here, we have characterized the cytoplasmic α-synuclein aggregates using a fractionation procedure with which different aggregate species can be separated. Overexpression of α-synuclein in cells produce two distinct types of aggregates; large juxtanuclear inclusion body and small punctate aggregates scattered throughout the cytoplasm. Biochemical fractionation results in an inclusion-enriched fraction and two small aggregate fractions. Electron microscopy and thioflavin S reactivity of the fractions show that the juxtanuclear inclusion bodies are filled with amyloid-like α-synuclein fibrils, whereas both the small aggregate fractions contain non-fibrillar spherical aggregates with distinct size distributions. These aggregates appear sequentially, with the smallest population appearing the earliest and the fibrillar inclusions the latest. Based on the structural and kinetic properties, we suggest that the small spherical aggregates are the cellular equivalents of the protofibrils. The proteins that co-exist in the Lewy bodies, such as proteasome subunit, ubiquitin, and hsp70 chaperone, are present in the fibrillar inclusions but absent in the protofibrils, suggesting that these proteins may not be directly involved in the early aggregation stage. As predicted in the aggresome model, disruption of microtubule with nocodazole reduced the number of inclusions and increased the size of the protofibrils. Despite the increased size, the protofibrils remained non-fibrillar, suggesting that the deposition of the protofibrils in the juxtanuclear region is important in the fibril formation. This study provides the evidence that the cellular fibrillation also involves non-fibrillar intermediate

species, and microtubule-dependent inclusion-forming process is required for the protofibril-to-fibril conversion in cells.

Introduction

A group of human neurodegenerative diseases, such as Parkinson's disease (PD)[1], dementia with Lewy bodies (LBs), and multiple system atrophy, are characterized by cytoplasmic inclusion bodies that are mainly composed of α-synuclein fibrils (1,2). While direct role of fibrils and the inclusion bodies in the disease pathogenesis is the subject of intense debate, an increasing body of evidence suggests that the *processes* of fibrillation and inclusion formation are closely related to the disease mechanism. First, two missense mutations (A53T and A30P) that are responsible for the familial PD has been identified in α-synuclein gene (3,4), and the mutant proteins have greater propensity for the self-association and aggregation than the wild-type protein (5-7). Indeed, both mutations accelerated the formation of the pre-fibrillar oligomers in vitro, whereas the fibril formation was slowed by one of the mutation (7,8). Second, transgenic animal models that were generated by the overexpression of human α-synuclein developed neuronal cytoplasmic inclusion bodies along with neuronal cell loss and behavioral defects (9-13). Some of these animals produce fibrillar inclusions (9,12), but others generate only the granular aggregates (10). In rat Parkinson's model that was established by a systemic administration of rotenone, nigrostriatal degeneration and the motor symptoms were also accompanied by α-synuclein-positive inclusion bodies (14). Therefore, cellular mechanism of α-synuclein aggregation is likely to be linked to at least some aspects of the disease process. Although the process of α-synuclein fibril formation has been implicated in the pathogenesis of PD by genetic and biochemical

evidence, the exact mechanism by which the processes of α-synuclein fibrillation and inclusion body formation contribute to neurodegeneration is currently unknown.

In dilute solution, α-synuclein does not have stable structure (15) except for some residual helical structure in the N-terminus of the protein (16). Fibrillation of α-synuclein is a nucleation-dependent process (17) and is initiated by acquiring a partially folded conformation (18), which is subsequently stabilized by self-association (19). Prior to the formation of fibril, the end product of the process, several non-fibrillar oligomeric aggregates, or protofibrils, were identified (20). Earliest and most common protofibrillar species are in a spherical shape with average height of 4.2 nm in case of wild type protein (21). The spherical protofibrils are thought to undergo head-to-tail associations to form elongated chain-like (22), and ring-like protofibrillar species (21). In their search for a potential pathogenic mechanism for α-synuclein protofibrils, Lansbury and colleagues demonstrated that only protofibrillar α-synuclein bind tightly and permeabilize synthetic vesicles in a size selective manner (23,24), suggesting membrane disruption via a pore-like mechanism. This hypothesis is supported by the findings that the two pathogenic mutations (A53T and A30P) promote the formation of annular pore like protofibrils (25) and result in an increased permeabilization activity relative to the wild type protein (24). Although some of the basic processes of α-synuclein aggregation, including the protofibrils with different morphologies, have been characterized in vitro, little is known about the fibrillation process or the intermediate protofibrillar species in cells.

In order to understand the mechanism of α-synuclein aggregation in cells, the following questions need to be addressed. (i) What is the end product of α-synuclein aggregation process in cells? (i.e., is it the fibril or other aggregate form?) (ii) What are the intermediates that proceed α-synuclein fibrillation in cells? (iii) Is the fibrillation process linked to the inclusion formation process and if so, how? Here, using a combination of biochemical fractionation, immunofluorescence labeling, and electron microscopy (EM), we show that cells produce inclusion bodies that are filled with α-synuclein fibrils. Before the appearance of the fibrillar inclusions, small non-fibrillar aggregates are formed, and the basic properties of these aggregates suggest that they are the cellular equivalent of the protofibrils. Our study also provides evidence that the inclusion-forming process, which is characterized by the transport of α-synuclein protofibrils and other cellular components to the pericentriolar region, is required for the conversion of protofibrils to fibrils.

Materials and Methods

Expression of human α-synuclein and induction of aggregation

Transformed African monkey kidney cell line COS-7 was maintained in Dulbecco's modified Eagle's medium (HyClone Laboratories, Inc., Logan, UT) with 10% fetal bovine serum (Hyclone Laboratories, Inc.) in a 37°C/5% CO_2 humidified incubator. To express α-synuclein, COS-7 cells were split on 100mm tissue culture dishes 1 day prior to infection to obtain ~90% confluence on the day of infection. For infection, adeno/α-syn (26) was added to each dish at a multiplicity of infection (MOI) of 75. After 90 minutes of incubation at 37°C, 9 ml of fresh medium was added and the cells were maintained at 37°C. The cells were then split the next day to ~40% confluence and maintained for another 48 hours or as indicated. Note that in our culture condition, time-course of aggregation varies depending on the size of the culture dish used. For example, cells cultured in 100 mm dish show more rapid aggregation than the cells in smaller dishes.

Fractionation of α-synuclein aggregates from COS-7 cells

COS-7 cells expressing α-synuclein were washed twice with cold phosphate-buffered saline (PBS) before addition of buffer T [20 mM Tris, pH 7.4, 25 mM KCl, 5 mM $MgCl_2$, 0.25 M sucrose, 1% Triton X-100, protease inhibitor cocktail (Sigma)] to each dish. After 5 min incubation at room temperature, the supernatant containing Triton-soluble proteins was carefully removed from plates. After gentle washing of dishes with PBS, the Triton-insoluble materials were scraped in buffer N (0.1 M Na_2CO_3, pH 11.5,

protease inhibitor cocktail), resuspended by repeated pipetting, and incubated on ice for 5 min. The extract was then centrifuged at 80 g for 10 min. The pellet containing big inclusions was resuspended in 1x Laemmli sample buffer (SB) for Western blot analysis, in PBS for immunofluorescence staining, or in 0.1 M phosphate buffer for EM. The supernatant containing small aggregates was then overlaid onto a discontinuous density gradient of 2.5%, 25%, and 35% iodixanol solutions (3 : 3: 1) in buffer T and centrifuged at 50,000 g for 30 min. The fractions were obtained from the top of the gradient, diluted with 2 volumes of PBS, and centrifuged at 16,000 g for 10 min. The pellets from fractions were then resuspended in 1x SB for Western blot analysis, in PBS for immunofluorescence staining, or in 0.1 M phosphate buffer for EM.

Western blotting

Western blot analysis was performed according to the procedure described in Lee et al. (27). LB509 monoclonal anti-α-synuclein antibody was purchased from Zymed Laboratories (South San Francisco, CA),

Immunofluorescence staining of cells and aggregate fractions

The procedure for cell staining has been described elsewhere (26). Briefly, cells grown on poly-L-lysine coated coverslips were fixed in 4% paraformaldehyde and permeabilized with 0.1% Triton X-100. Coverslips were then blocked in blocking solution (PBS, 5% bovine serum albumin, 3% goat serum). Primary antibodies in blocking solution were added at dilutions described below and incubated for 30 min: LB509 monoclonal α-synuclein antibody (1:1000; Zymed), 7071 polyclonal α-synuclein

antibody (1:1000; provided by Peter Lansbury at Harvard Medical School, Boston, MA), anti-ubiquitin antibody (1:1000; Chemicon), anti-Hsp70/Hsc70 antibody (1:200; StressGen), anti-20S proteasome α-subunit antibody (1:200; Calbiochem-Novabiochem Corp., San Diego, CA). Coverslips were extensively washed for 1~1.5 hours with PBS before addition of fluorescent dye (Cy3, Cy2, Rhodamine Red X)-conjugated goat anti-mouse or anti-rabbit antibodies (Jackson ImmunoResearch Laboratories, Inc., West Grove, PA, 1:500) in blocking solution for 30 min. Thioflavin S (Sigma) staining and Hoechst 33258 (Molecular Probes, Inc., Eugene, OR) staining were performed according to Lee et al. (26). For staining of obtained fractions, the samples in PBS were placed on coverslips and let partially dry. After fixing the coverslips in 4% paraformaldehyde in PBS for 30 min, the staining was done in the same manner as described above.

Electron microscopy

COS-7 cells expressing α-synuclein and α-synuclein fractions in PBS were prepared for section as described in Bouley et al. (28). For the immunolabeling, the sections were incubated in 1% gelatin in PBS and then in 0.03 M glycine in PBS. After blocking in 2% BSA in PBS, the sections were incubated with LB509 antibody (1:250) in 2% BSA in PBS, followed by 10nm gold-conjugated goat anti-mouse IgG antibody. The sections were stained with 1% uranyl acetate and lead citrate.

For negative staining of fibrils from the inclusion bodies, the pellet from 80 g spin was rinsed and then resuspended in PBS and incubated in 1% SDS for 20 min at room temperature. After the incubation, the sample was centrifuged at 80 g to remove undissolved inclusion bodies, and the supernatant was centrifuged at 100,000 g for 30

min. The pellet was then resuspended in 50 mM Tris, pH 7.4 and then placed on a carbon-coated grid. The grid was incubated with LB509 antibody (1:250), followed by goat anti-mouse IgG antibody conjugated with 10nm gold particle, and after two rinses with distilled water, it was stained with 1% uranyl acetate. The images were obtained from Philips CM 12 electron microscope.

Results

To characterize the cytoplasmic α-synuclein aggregates, we established a mammalian cell culture model using COS-7 cells and recombinant adenoviral vector. In this model, expression of monomer is saturated at the MOI of around 25, and higher expression over the saturation point induces the spontaneous aggregation, which shows exponential increase with respect to the increasing MOI^2. Alternatively, inhibitors of mitochondrial respiratory chain, such as rotenone, greatly enhance α-synuclein aggregation even at the expression level slightly above the saturation point (MOI of 35), in which the spontaneous aggregation is minimal (26). In this study, the spontaneous α-synuclein aggregation was induced in COS-7 cells at the MOI of 75, and the resulting cytoplasmic aggregates were characterized using biochemical fractionation combined with imaging analyses.

Similar to what was observed in the rotenone-induced α-synuclein aggregation (26), spontaneous aggregation at MOI 75 resulted in two types of aggregates that are distinct in their sizes and cytoplasmic distributions. One type is represented by small punctate aggregates that are dispersed throughout the cytoplasm, and the other is large juxtanuclear inclusion bodies (Fig 1). The juxtanuclear inclusion bodies bind to thioflavin S (Fig. 1B), a fluorescent dye specific for the highly ordered cross β-sheet structure, thus an indicative of the amyloid-like fibrillar structures (see below for the ultrastructural analysis). In contrast, the small punctate aggregates are thioflavin S-negative (Fig. 1A), indicating a non-fibrillar conformation. The difference in the dye

binding properties suggests that these two types of aggregates have different structural properties.

Fig. 1

Previous immunohistochemical studies of human LBs showed that they are also stained with ubiquitin (29), proteasomes (30), and molecular chaperones, such as hsp70 (11). To determine whether the inclusion bodies in our cell system contain these proteins, we co-stained the cells for α-synuclein with ubiquitin, α-subunit of 20S proteasome, or hsp70. Like human LBs, large juxtanuclear inclusion bodies were positive for all these proteins (Fig. 1 B). On the other hand, most of peripheral punctate aggregates were not stained with ubiquitin, the proteasome subunit, or hsp70 (Fig. 1A). Interestingly, the cells with small punctate aggregates display brighter staining in the perinuclear region for ubiquitin, hsp70, and 20S α-subunit proteins than the cells without aggregates (data not shown), where they show some degree of co-localization with α-synuclein punctate aggregates (Fig 1A). Mitochondria and lysosomes are also elevated and accumulated in the perinuclear region along with the small punctate α-synuclein aggregates[2]. The accumulation of these proteins and organelles that are required for the degradation of macromolecules in the perinuclear region, at what appears to be an early stage of inclusion formation, supports the hypothesis that the inclusion-forming process represents how the cells deliberately sequester and degrade abnormal protein aggregates at the specialized subcellular location.

In order to further characterize different types of α-synuclein aggregates, we have established a procedure by which these aggregates are separated into different fractions (Fig. 2A). Cells that produce α-synuclein aggregates were extracted with 1% Triton X-100 in the culture dish, and the Triton-soluble proteins were gently removed. Under this condition, the soluble monomeric α-synuclein was completely removed, and the aggregates were remained in the culture dish, probably due to their association with unknown structures. The remaining Triton-insoluble portion was then scraped in basic pH buffer, in which the aggregates were dissociated from the cellular structures, and centrifuged at 80 g. After the centrifugation at 80 g for 10 min, the pellet fraction was found to contain exclusively the large inclusion bodies, whereas the supernatant contained predominantly small α-synuclein aggregates (see below). In an attempt to further separate the different α-synuclein aggregates, the supernatant was then subjected to a density gradient centrifugation as described in Fig. 2A. Western blot analysis of the fractions (frs) has identified three distinct fractions containing SDS-resistant α-synuclein aggregates (fr 2, fr 4, and 80 g pellet) (Fig. 2B). Although fr 7 also contains α-synuclein aggregates in some cases, immunofluorescence and immuno-EM studies suggested that this fraction consists of clumps of heterogeneous α-synuclein aggregates, which appear to be a mixture of the aggregates found in fr 2 and fr 4 (data not shown).

Fig. 2

Dual fluorescence labeling shows that the fr 2, and fr 4 contain small punctate aggregates that are thioflavin S-negative, whereas the 80 g pellet contains large inclusion bodies that

are thioflavin S-positive (Fig. 3A), confirming the in situ immunofluorescence results (Fig. 1). Also consistent with the in situ immunofluorescence staining, the small aggregates do not contain ubiquitin, hsp70, or 20S proteasome α-subunit, whereas the large inclusion bodies in the 80 g pellet were positive for these proteins (Fig. 3B, C, and D). The inclusion bodies were found exclusively in the 80 g pellet. These results confirm that the cells produce different types of α-synuclein aggregates with distinct conformational and compositional properties and that the separation of these aggregates can be achieved using our procedure.

Fig. 3

To further analyze the ultrastructural features of α-synuclein aggregates, the fractions were examined by immuno-EM. The aggregates in both the fr 2 and fr 4 appear to be non-fibrillar spheres (Fig. 4A and B). To compare the size distributions of aggregates in fr 2 and fr 4, we measured the diameter of each aggregate labeled with α-synuclein antibody (Fig. 4C). Those aggregates that are irregular in shape were measured across the longest and shortest axes, and the median value was calculated. Random measurement of the diameter of these spheres shows the different size distributions in these fractions, and the calculated mean diameters for fr 2 and fr 4 were 24 nm and 34 nm, respectively.

Fig. 4

EM analysis confirmed that the large inclusion bodies were enriched in the 80 g pellet and they were immunostained with α-synuclein antibody (Fig. 5A). However, in contrast to the small spherical aggregates in fr 2 and fr 4, the inclusions are filled with fibril structures. To further characterize the fibrils of these inclusion bodies, the 80 g pellet was disrupted in 1% SDS and the released fibrils were collected by 100,000 g centrifugation. The fibrils isolated from the inclusions are 8-13 nm in width and are clearly labeled with α-synuclein antibody (Fig. 5B). These fibrils resemble the ones isolated from human LBs (29) or the inclusions of the transgenic mice (12). Thicker structures, which appear to be fibril bundles, are also frequently observed (Fig. 5C). These ultrastructural morphologies, along with the thioflavin S binding property, demonstrate that α-synuclein aggregation process in our cell model produces the inclusion bodies that are composed of α-synuclein fibrils, thus suggesting that this process of inclusion body formation in these cells may resemble the process of LB formation in human brain.

Fig. 5

To gain insights into dynamic relationship between different aggregate species, we investigated the time-dependent formation of the small spherical aggregates and the fibrillar inclusions in the 80 g supernatant and pellet fractions, respectively. As shown in Fig. 6A, the small aggregates in the 80 g supernatant became apparent as early as 48 h post-infection and increased with time. On the other hand, the fibrillar inclusions in the 80 g pellet did not appear until 60 h (Fig. 6A). This result suggests that the small

spherical aggregates are formed before the formation of fibrillar inclusions. We then investigated the time-course for the two subspecies of spherical aggregates. Fractionation of the spherical aggregates at different time points shows that the fr 2 aggregates are the earliest species formed, appearing at 48 h (Fig. 6B, top panel). The fr 4 aggregates were formed slightly later at around 54 h (Fig. 6B, second panel). Both species increased progressively at later time points, but the increase was more dramatic for the fr 4 aggregates (Fig. 6B). The fact that these two fractions show differences in both the time of appearance and the rate of increase suggests that they are distinct aggregate species and that the fr 2 aggregates may be the precursors for the fr 4 aggregates.

Fig. 6

It has been demonstrated with a number of proteins that the juxtanuclear inclusion formation requires the microtubule-dependent transport of peripheral small aggregates to the pericentriolar region (31,32). To test if microtubule-dependent transport is important for the formation of α-synuclein inclusion body, we treated the cells with a microtubule-disrupting agent, nocodazole, and assessed the inclusion formation in two ways. First, the number of inclusion bodies was counted after the immunofluorescence staining (Fig. 7A). Second, the relative amounts of inclusion bodies and small non-fibrillar aggregates were measured after the fractionation (Fig. 7B). Both analyses clearly show the decrease of the inclusion bodies after nocodazole treatment, implicating the importance of microtubule-dependent transport system in the inclusion formation. Furthermore, the fractionation experiment shows that the reduction of inclusion bodies is accompanied by

the increase of the small aggregates (Fig. 7B), confirming that nocodazole inhibits the transport of the small aggregates rather than the aggregation per se. Interestingly, when the microtubule is disrupted, bigger foci were frequently found in the periphery of the cell (Fig. 7C), which implies that the peripheral aggregates can grow bigger to a certain extent, if their transport to the pericentriolar region is blocked. This finding raised a question as to whether the large foci that are grown in the periphery of the cell can acquire the characteristics of the juxtanuclear inclusion bodies. To address this question, we have investigated the thioflavin S binding property and the immunoreactivities for the proteins that are found in the inclusion bodies. Unlike the juxtanuclear inclusion bodies, the large peripheral foci are thioflavin S-negative, indicating non-fibrillar nature of the aggregates, and devoid of ubiquitin, hsp70, and 20S proteasome α-subunit (Fig. 7C). These data suggest that fibrillation and acquisition of the auxiliary proteins are not spontaneous consequences of the aggregate growth, rather they are closely linked to the microtubule-dependent inclusion-forming process.

Fig 7

Discussion

In our previous study, we have demonstrated that overexpression of α-synuclein or exposure of cells to mitochondrial inhibitors produces two distinct forms of α-synuclein aggregate; small punctate aggregates that are scattered throughout the cytoplasm and large juxtanuclear inclusion bodies. Here, we have characterized the structural natures of these aggregates and investigated the relationship between them in the context of inclusion forming process. Using biochemical fractionation and EM analysis, we have demonstrated small aggregates are non-fibrillar spheres, and the inclusion bodies are filled with α-synuclein fibrils. Time-dependent analysis shows that small non-fibrillar aggregates precede the formation of fibrillar inclusions. An anti-microtubule agent, nocodazole, causes a reduction in the number of fibrillar inclusions and the accumulation of non-fibrillar aggregates in the cytoplasm, suggesting that these non-fibrillar aggregates are the precursors of the fibrillar aggregates in the inclusion bodies. Protofibrils are described as non-fibrillar aggregates that precede the fibril formation and are often enriched with β-sheet structure (20). Although the conformational characteristics of the cytoplasmic aggregates are not yet available, the ultrastructural and kinetic properties suggest that the small non-fibrillar aggregates are the cellular equivalents of the protofibrils.

In solution, fibrillation of α-synuclein, which involves a number of metastable intermediate species including various protofibrils, is a continuous process, because all the monomers and assembly intermediates are freely diffusible and available for the

molecular interactions. However, in cells, fibrillar α-synuclein aggregates are found exclusively in the juxtanuclear inclusions, and interfering with the transport of protofibrils to the pericentriolar region inhibits the fibril formation. These findings support the hypothesis that monomer to protofibril conversion and protofibril to fibril conversion are spatially separate processes; the former seems to be a diffusion-limited reaction and occur throughout the cytoplasm, whereas the latter is restricted only in the pericentriolar region. In cells, the protofibrils seem to be associated with detergent-insoluble structures (H-J Lee and S-J Lee, unpublished data), which limits their chance to interact with one another. When microtubule-mediated transport is disrupted with nocodazole, peripheral protofibrils become larger than normal but do not turn into fibrils. Thus, it is only after the protofibrils are transported and deposited in the pericentriolar region that the interactions between the protofibrils are allowed to undergo the transformation into fibrils.

Protofibrillar intermediates (often in a spherical morphology) have been found in virtually all fibrillation characterized, thus becoming a universal mechanism of amyloid-like fibril formation (33-36). However, the mechanism of the protofibril-to-fibril transition is not clearly understood. In vitro, most α-synuclein protofibrils are either in a spherical shape or in the morphologies (chain-like and annular pore-like structures) that appear to be produced by the association of the spherical protofibrils (20,21). This observation implies that the protofibril spheres can self-associate to form higher-order structures. Similar mechanism has been proposed in the fibrillation of sup35 protein (N-terminal and mid-domain fragment) in which oligomer-oligomer interactions precede the

conformational changes to amyloid-like fibrils (34). Our observation that the fibril formation occurs only when the protofibrils are concentrated and allowed to interact with one another also supports the possibility that the fibril formation in vivo could be driven by protofibril-protofibril interactions. However, our findings do not exclude the role of monomer in cellular fibrillation process. Direct incorporation of monomer into the fibrils could also play a role in fibril growth in vivo. In vitro studies show that when the protofibrils are populated in solution, the transition from spherical aggregates to the amyloid-like fibrils is a spontaneous process. However, in cells, this process may be assisted by the proteins that are co-accumulated with α-synuclein aggregates in the pericentriolar region, such as molecular chaperones.

Microtubule-dependent deposition of peripheral aggregates into pericentriolar region has been documented with several other proteins, and the resulting inclusion bodies are referred to as aggresomes (37,38). Aggresome represents one of the end-points of cellular responses to misfolded proteins, with other competing end-points being degradation and refolding. Although many proteins share the same mechanism for the deposition in the pericentriolar region, the physical states of the final aggregated forms seem to be determined by the conformational properties of individual proteins. For example, aggregates of cystic fibrosis transmembrane conductance regulator (CFTR) (31) or GFP-250 (32) remain granular in shape, while α-synuclein aggregates are transformed into fibrils after deposition in the aggresomes. If the recent proposal that protofibrils are the pathogenic species (20) is correct, accelerating the transformation of disease-associated protofibrils into fibrils would have evolutionary advantage. Developing

noninvasive ways to interfere with the transport of protofibrils to the inclusion-forming site or the structural transition to fibrils will allow us to assess the role of these processes in α-synuclein-mediated cell death.

Inclusion bodies, either the ones that are produced in our cell system or LBs in human brain, contain protein components other than α-synuclein fibrils, such as proteasome subunits (30), ubiquitin (29), and molecular chaperones (11). Their presence in inclusion bodies raised the question of whether they co-aggregate with α-synuclein, or even promote the aggregation process. Our study shows that α-synuclein protofibrils, both the ones in the cells or isolated from the cells, are not stained for these proteins, but they are co-deposited in the perikaryal region with α-synuclein protofibrils. In a previous study, we have shown that early stage α-synuclein oligomerization in crude cytosol preparation is highly self-selective (19). In agreement with our findings, Rajan et al. have recently demonstrated that aggregation of misfolded proteins is the result of highly specific self-association, rather than non-specific interactions between unrelated proteins (39). Therefore, it is unlikely that the proteins that co-exist in the inclusion bodies play a direct role in promoting α-synuclein aggregation. Rather, it seems more likely that the presence of protein degradation machineries and the molecular chaperones is an indication of cell's attempt to clear these protein deposits.

Fractionation of protofibrillar aggregates resulted in the separation of two subspecies with distinct size distribution. It is not entirely clear at the moment whether they represent two distinct intermediates in a linear process or one of them is an artificial

outcome that are formed during the extraction procedure, such as fragmentation of larger aggregates to smaller pieces or large clumps of aggregates due to an incomplete resuspension. If they were the same species, it would be predicted that their kinetic behavior is identical. However, our time-course experiment shows that these two species have clearly distinctive kinetics; smaller species appears first, followed by the larger one. Thus, it is likely that they are distinct entities and may be related in a linear process.

In conclusion, we have demonstrated that α-synuclein fibrillation is tightly associated with the microtubule-dependent inclusion-forming process, which seems to be necessary for the protofibril-to-fibril transition. The ability to separate different species and semi-quantitatively analyze them will allow the detailed characterization of the α-synuclein aggregation process in cells.

Acknowledgments

We thank P. Lansbury for reading the manuscript, H. Lashuel for his critical comments, S. Patel for technical assistance, and N. Ghori for the assistance for EM.

References

1. Trojanowski, J. Q., Goedert, M., Iwatsubo, T., and Lee, V. M. (1998) *Cell Death Differ* **5,** 832-7
2. Goedert, M. (2001) *Nat Rev Neurosci* **2,** 492-501.
3. Polymeropoulos, M. H., Lavedan, C., Leroy, E., Ide, S. E., Dehejia, A., Dutra, A., Pike, B., Root, H., Rubenstein, J., Boyer, R., Stenroos, E. S., Chandrasekharappa, S., Athanassiadou, A., Papapetropoulos, T., Johnson, W. G., Lazzarini, A. M., Duvoisin, R. C., Di Iorio, G., Golbe, L. I., and Nussbaum, R. L. (1997) *Science* **276,** 2045-7
4. Kruger, R., Kuhn, W., Muller, T., Woitalla, D., Graeber, M., Kosel, S., Przuntek, H., Epplen, J. T., Schols, L., and Riess, O. (1998) *Nat Genet* **18,** 106-8
5. Conway, K. A., Harper, J. D., and Lansbury, P. T. (1998) *Nat Med* **4,** 1318-20
6. Narhi, L., Wood, S. J., Steavenson, S., Jiang, Y., Wu, G. M., Anafi, D., Kaufman, S. A., Martin, F., Sitney, K., Denis, P., Louis, J. C., Wypych, J., Biere, A. L., and Citron, M. (1999) *J Biol Chem* **274,** 9843-6
7. Li, J., Uversky, V. N., and Fink, A. L. (2001) *Biochemistry* **40,** 11604-13.
8. Conway, K. A., Lee, S. J., Rochet, J. C., Ding, T. T., Williamson, R. E., and Lansbury, P. T., Jr. (2000) *Proc Natl Acad Sci U S A* **97,** 571-6
9. Feany, M. B., and Bender, W. W. (2000) *Nature* **404,** 394-398
10. Masliah, E., Rockenstein, E., Veinbergs, I., Mallory, M., Hashimoto, M., Takeda, A., Sagara, Y., Sisk, A., and Mucke, L. (2000) *Science* **287,** 1265-1269

11. Auluck, P. K., Chan, H. Y., Trojanowski, J. Q., Lee, V. M., and Bonini, N. M. (2002) *Science* **295,** 865-8.

12. Giasson, B. I., Duda, J. E., Quinn, S. M., Zhang, B., Trojanowski, J. Q., and Lee, V. M.-Y. (2002) *Neuron* **34,** 521-533

13. Lee, M. K., Stirling, W., Xu, Y., Xu, X., Qui, D., Mandir, A. S., Dawson, T. M., Copeland, N. G., Jenkins, N. A., and Price, D. L. (2002) *Proc Natl Acad Sci U S A* **99,** 8968-73.

14. Betarbet, R., Sherer, T. B., MacKenzie, G., Garcia-Osuna, M., Panov, A. V., and Greenamyre, J. T. (2000) *Nat Neurosci* **3,** 1301-6.

15. Weinreb, P. H., Zhen, W., Poon, A. W., Conway, K. A., and Lansbury, P. T., Jr. (1996) *Biochemistry* **35,** 13709-15

16. Eliezer, D., Kutluay, E., Bussell, R., Jr., and Browne, G. (2001) *J Mol Biol* **307,** 1061-73.

17. Wood, S. J., Wypych, J., Steavenson, S., Louis, J. C., Citron, M., and Biere, A. L. (1999) *J Biol Chem* **274,** 19509-12

18. Uversky, V. N., Li, J., and Fink, A. L. (2001) *J. Biol. Chem.* **276,** 10737-44.

19. Uversky, V. N., Lee, H. J., Li, J., Fink, A. L., and Lee, S. J. (2001) *J Biol Chem* **5,** 5

20. Goldberg, M. S., and Lansbury, P. T., Jr. (2000) *Nature Cell Biol.* **2,** E115-E119

21. Ding, T. T., Lee, S.-J., Rochet, J. C., and Lansbury, P. T. (2002) *Biochemistry* in press

22. Conway, K. A., Harper, J. D., and Lansbury, P. T., Jr. (2000) *Biochemistry* **39,** 2552-63

23. Volles, M. J., Lee, S. J., Rochet, J. C., Shtilerman, M. D., Ding, T. T., Kessler, J. C., and Lansbury, P. T., Jr. (2001) *Biochemistry* **40,** 7812-9.

24. Volles, M. J., and Lansbury, P. T., Jr. (2002) *Biochemistry* **41,** 4595-602.

25. Lashuel, H. A., Hartley, D., Petre, B. M., Walz, T., and Lansbury, P. T. (2002) *Nature* **418,** 291.

26. Lee, H. J., Shin, S. Y., Choi, C., Lee, Y. H., and Lee, S. J. (2002) *J Biol Chem* **277,** 5411-7.

27. Lee, S.-J., Liyanage, U., Bickel, P. E., Xia, W., Lansbury, P. T., Jr., and Kosik, K. S. (1998) *Nat. Med.* **4,** 730-734

28. Bouley, D. M., Ghori, N., Mercer, K. L., Falkow, S., and Ramakrishnan, L. (2001) *Infect Immun* **69,** 7820-31.

29. Spillantini, M. G., Crowther, R. A., Jakes, R., Hasegawa, M., and Goedert, M. (1998) *Proc Natl Acad Sci U S A* **95,** 6469-73

30. Ii, K., Ito, H., Tanaka, K., and Hirano, A. (1997) *J Neuropathol Exp Neurol* **56,** 125-31.

31. Johnston, J. A., Ward, C. L., and Kopito, R. R. (1998) *J Cell Biol* **143,** 1883-98.

32. Garcia-Mata, R., Bebok, Z., Sorscher, E. J., and Sztul, E. S. (1999) *J Cell Biol* **146,** 1239-54.

33. Bucciantini, M., Giannoni, E., Chiti, F., Baroni, F., Formigli, L., Zurdo, J., Taddei, N., Ramponi, G., Dobson, C. M., and Stefani, M. (2002) *Nature* **416,** 507-11.

34. Serio, T. R., Cashikar, A. G., Kowal, A. S., Sawicki, G. J., Moslehi, J. J., Serpell, L., Arnsdorf, M. F., and Lindquist, S. L. (2000) *Science* **289,** 1317-21.

35. Harper, J. D., Wong, S. S., Lieber, C. M., and Lansbury, P. T., Jr. (1999) *Biochemistry* **38,** 8972-80.

36. Poirier, M. A., Li, H., Macosko, J., Cai, S., Amzel, M., and Ross, C. A. (2002) *J Biol Chem* **8,** 8

37. Kopito, R. R. (2000) *Trends Cell Biol* **10,** 524-30.

38. Garcia-Mata, R., Gao, Y. S., and Sztul, E. (2002) *Traffic* **3,** 388-396.

39. Rajan, R. S., Illing, M. E., Bence, N. F., and Kopito, R. R. (2001) *Proc Natl Acad Sci U S A* **98,** 13060-5.

Footnotes

[1] The abbreviations used are: PD, Parkinson's Disease; LB, Lewy body; MOI, multiplicity of infection; EM, electron microscopy; PBS, phosphate-buffered saline; SB, 1X Lammeli sample buffer; fr, fraction.

[2] N. Gosavi, H. -J. Lee, J.S. Lee, S. Patel, & S.-J. Lee, submitted for publication.

Figure legends

Fig.1 Dye-binding property and protein components of the different α-synuclein aggregate species in cells. α-Synuclein was overexpressed in COS-7 cells by recombinant adenoviral vector at MOI of 75. After 3 days post-infection, α-synuclein aggregates were co-stained with thioflavin S, ubiquitin, hsp70, or 20S proteasome α-subunit. Small punctate aggregates (A) and large juxtanuclear inclusion bodies (B) are shown. Note that the small α-synuclein aggregates are thioflavin S-negative and exclude the immunolabelings for ubiquitin, hsp70, or 20S proteasome α-subunit (A), whereas inclusion bodies are thioflavin S-positive and contain all these proteins (B). Nuclei are stained with Hoechst 33258 (blue).

Fig. 2 Separation of α-synuclein aggregates by density gradient centrifugation. (A) Schematic diagram of separation procedure. See "Materials and Methods" for details. (B) Western blotting of the fractions. Note that the fr 2 and fr 4 and the 80 g pellet contain α-synuclein aggregates. The stacking gel portion is indicated as a line on the right side of the gel.

Fig. 3 Dye-binding properties and protein compositions of fractionated α-synuclein aggregates. α-Synuclein aggregates in fr 2 and fr 4 and 80g pellet were co-stained for α-synuclein (red) with thioflavin S (A, green), ubiquitin (B, green), hsp70 (C, green), and 20S proteasome α-subunit (D, green). Only merged images of red and green are shown. Note that aggregates in fr 2 and fr 4 are thioflavin S-negative and do not contain the

proteins tested with a few exceptions, whereas the large inclusion bodies in 80 g pellet are thioflavin S-positive and stained for all the proteins tested here.

Fig. 4 ImmunoEM analysis of α-synuclein aggregates from the density gradient fractions. α-Synuclein aggregates in fr 2 (A) and fr 4 (B) were labeled with LB509 anti-α-synuclein antibody and 10 nm gold-conjugated secondary antibody. (C) Aggregate size distribution of each gradient fraction. The calculated mean diameters for fr 2 and fr 4 were 24 and 34 nm, respectively.

Fig. 5 Ultrastructural analysis of α-synuclein inclusion bodies in the 80 g pellet. (A) Inclusion bodies in the 80 g pellet were labeled with LB509 and 10 nm gold-conjugated secondary antibody. High magnification image of the boxed region on the left image is shown on the right. Note the fibril-like structures on the magnified image. (B, C) ImmunoEM images of individual fibrils (B) and fibril bundles (C). The α-synuclein inclusion bodies in the 80 g pellet were disrupted with 1% SDS and the released fibrils were labeled with LB509, followed by the staining with uranyl acetate.

Fig. 6 Time-dependent progression of α-synuclein aggregates (A) Non-fibrillar α-synuclein aggregates and inclusion bodies were obtained in the 80 g supernatant and the pellet, respectively, at times indicated, and analyzed with LB509 antibody. (B) Subspecies of non-fibrillar α-synuclein aggregates in the 80 g supernatant was further fractionated at times indicated. The stacking gel portion is indicated as a line on the right side of the gel.

Fig. 7 Nocodazole treatment inhibits the progression of peripheral α-synuclein aggregates into juxtanuclear fibrillar inclusions. (A) Percentage of cells with inclusion bodies. COS-7 cells overexpressing α-synuclein were treated with DMSO or nocodazole (10 μg/ml) for 48 hours before the immunofluorescence labeling for α-synuclein and counting. The numbers above each bar indicate the number of cells with inclusion bodies/ the total number of cells counted. For each sample, ten random fields were selected for counting. (B) Reduction in inclusion bodies and concomitant increase of small non-fibrillar aggregates after the nocodazole treatment. COS-7 cells expressing α-synuclein were treated with DMSO or nocodazole for 24 hours before extraction, and the aggregates were fractionated according to the procedure described in Fig. 2. The fractions were analyzed by Western blotting with LB509 antibody. The stacking gel portion is indicated as a line on the right side of the gel. Txsol; Triton X-100-soluble fraction -; DMSO +; nocodazole (C) Enlarged peripheral α-synuclein aggregates were found in the cells that were treated with nocodazole. These enlarged peripheral foci did not stain with thioflavin S or the antibodies against ubiquitin, hsp70, or 20S proteasome α-subunit.

Fig. 1 Lee

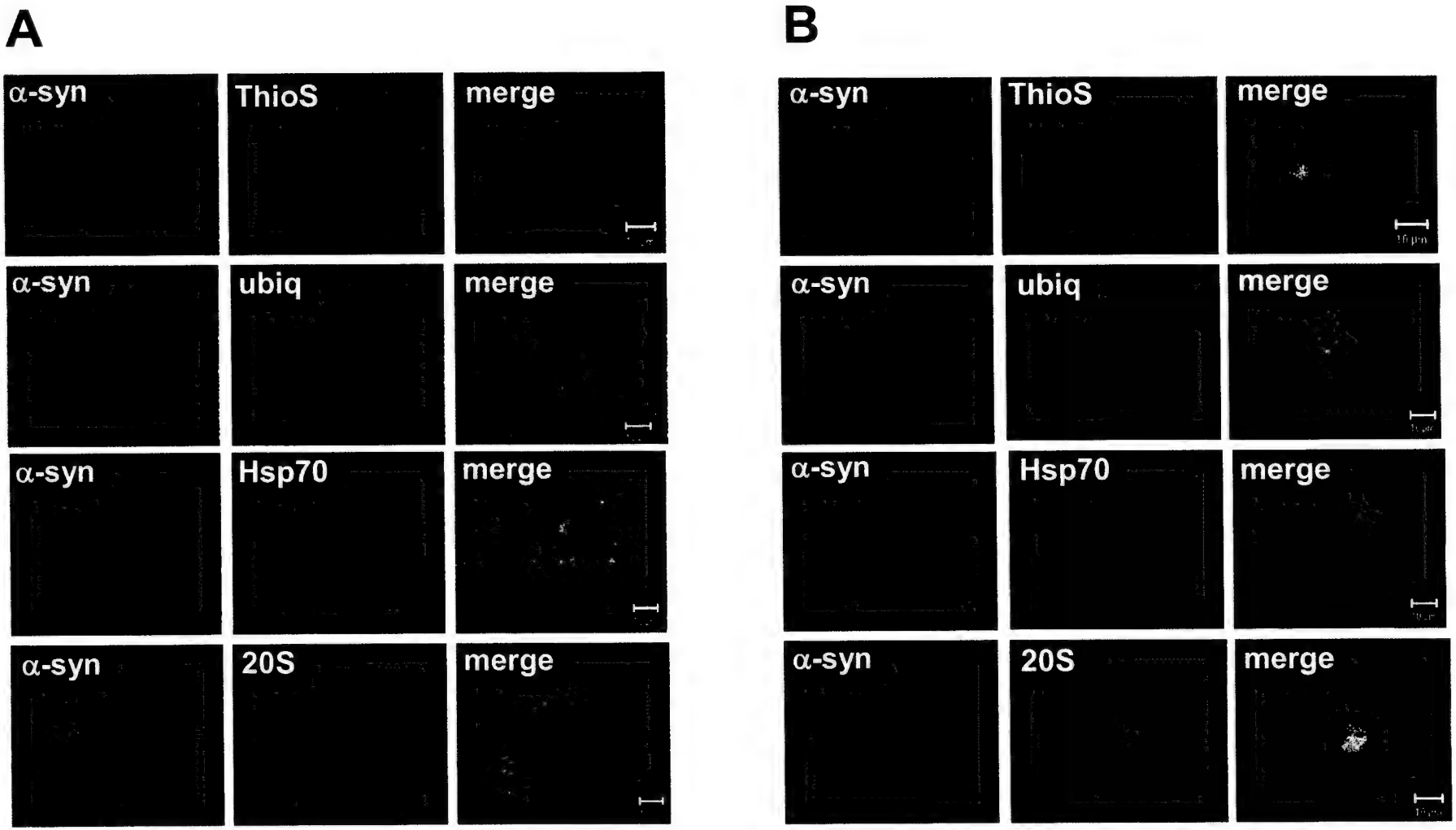
A
α-syn
ThioS
merge
α-syn
ubiq
merge
α-syn
Hsp70
merge
α-syn
20S
merge
B
α-syn
ThioS
merge
α-syn
ubiq
merge
α-syn
Hsp70
merge
α-syn
20S
merge

Fig 2. Lee

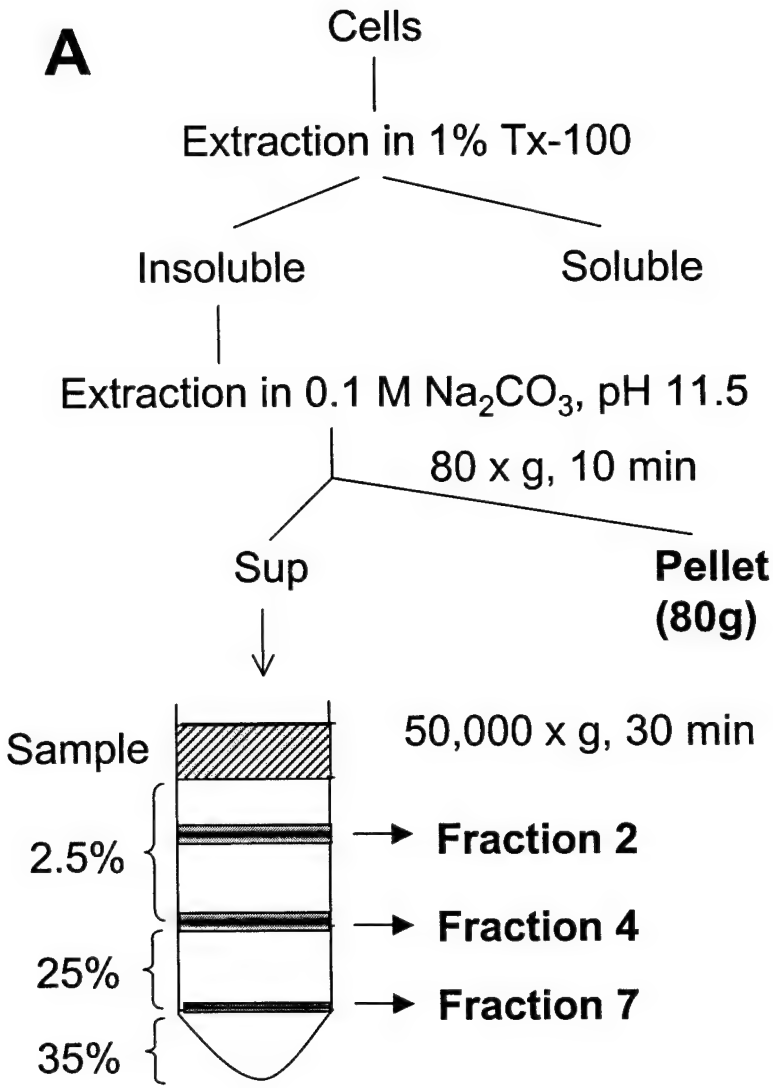
A
Cells
Extraction in 1% Tx-100
Insoluble
Soluble
Extraction in 0.1 M Na_2CO_3, pH 11.5
80 x g, 10 min
Sup
Pellet (80g)
Sample
50,000 x g, 30 min
2.5%
25%
35%
Fraction 2
Fraction 4
Fraction 7

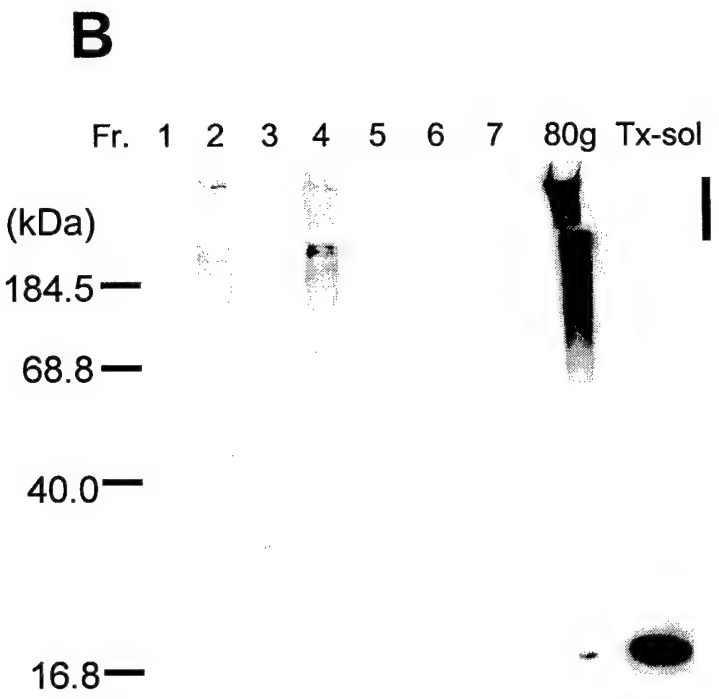
B
Fr. 1 2 3 4 5 6 7 80g Tx-sol
(kDa)
184.5
68.8
40.0
16.8

Fig 3. Lee

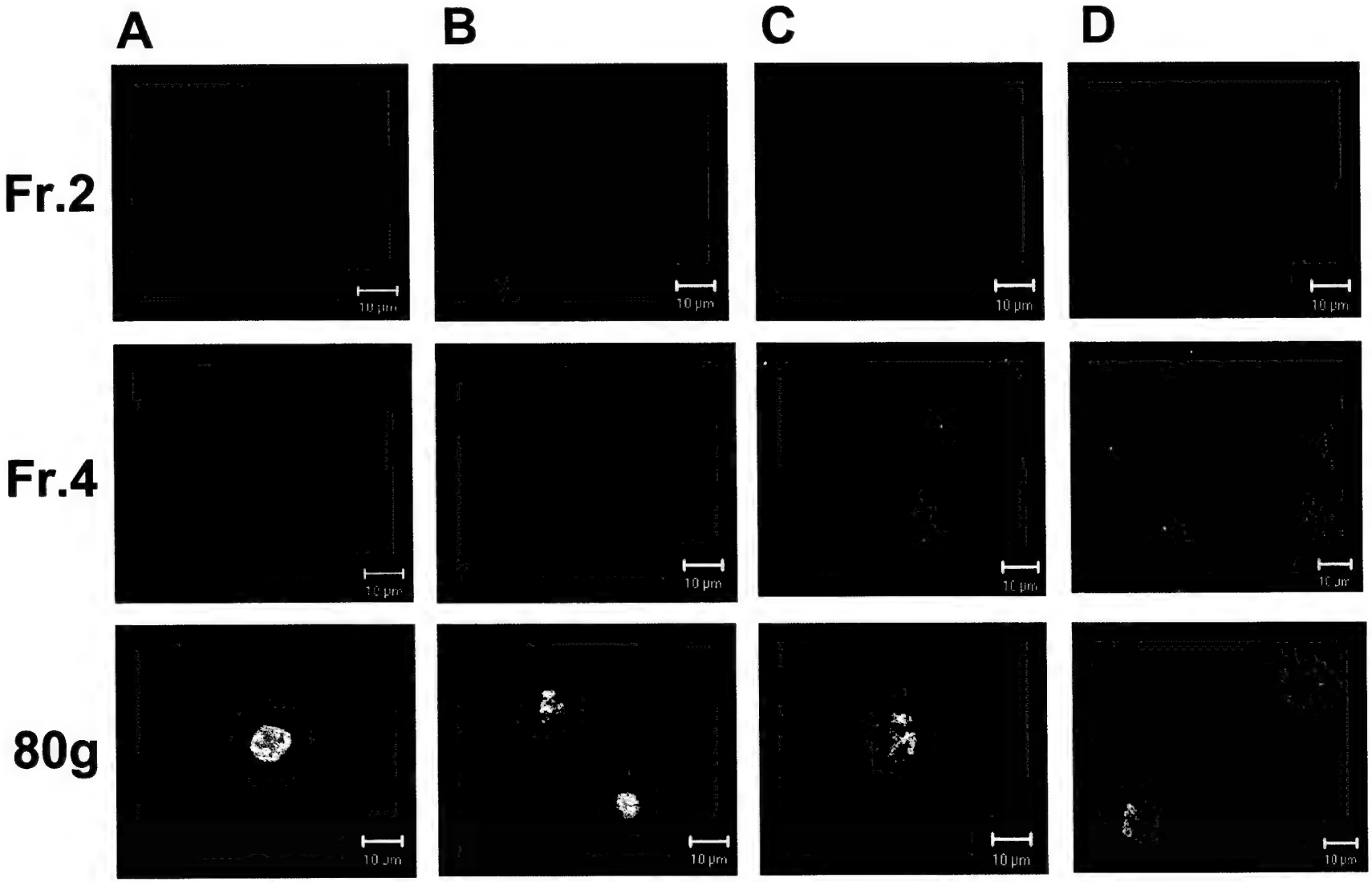

Fig 4. Lee

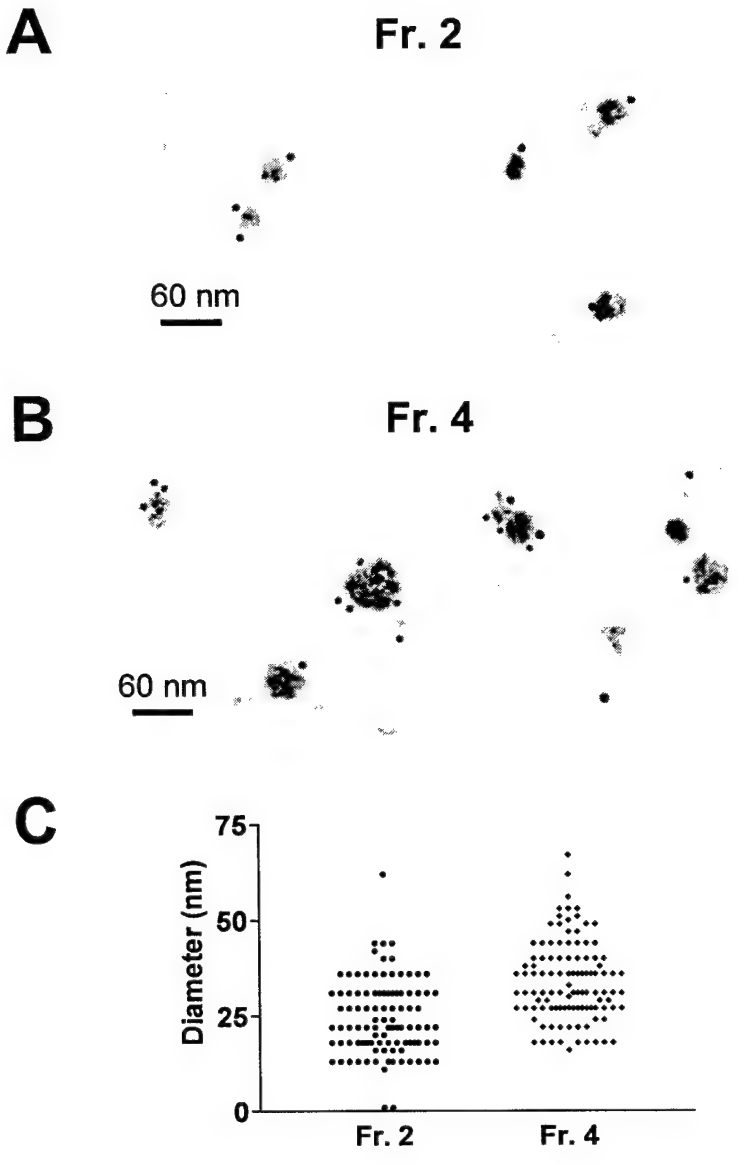

Fig 5. Lee

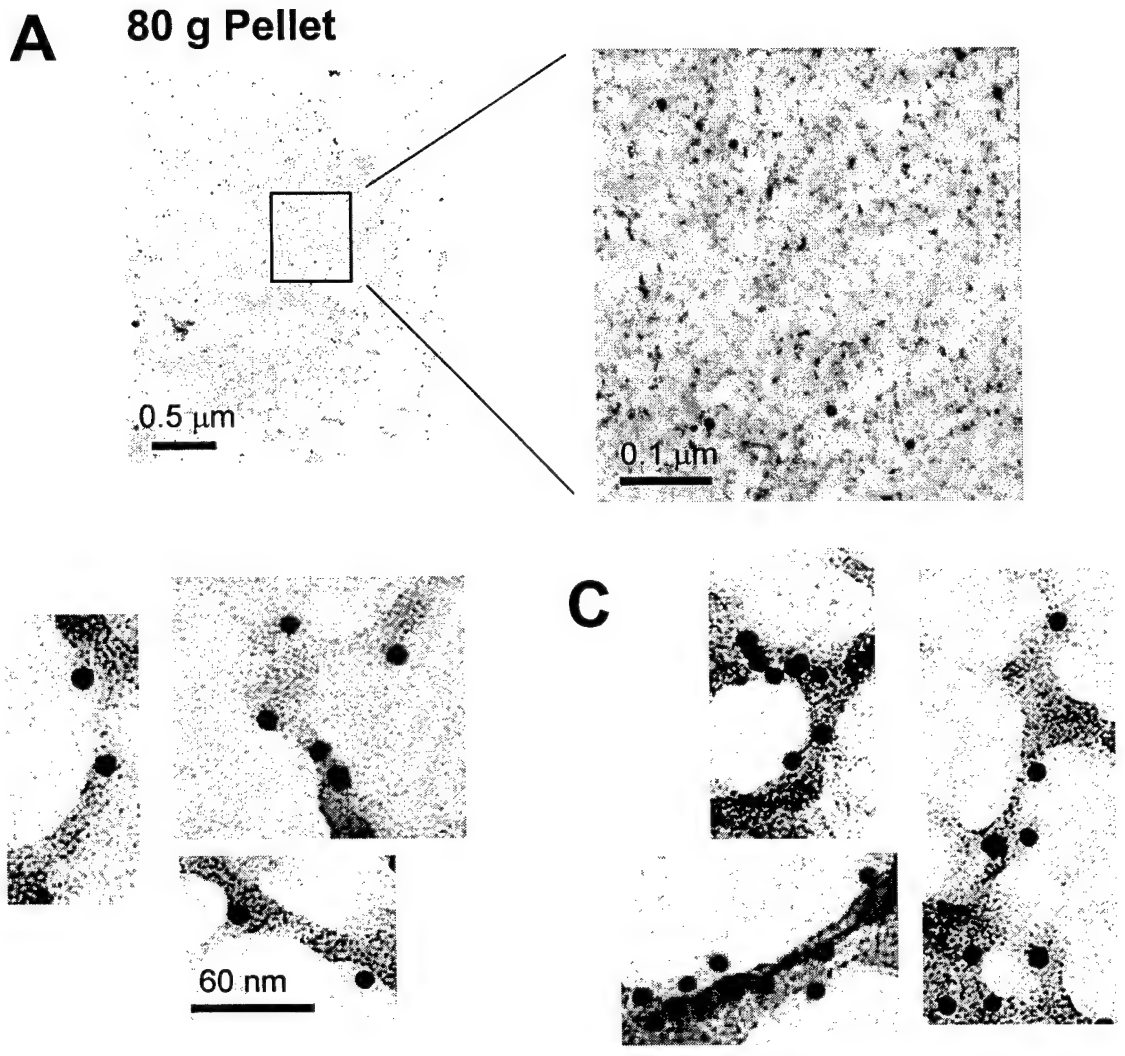

Fig 6. Lee

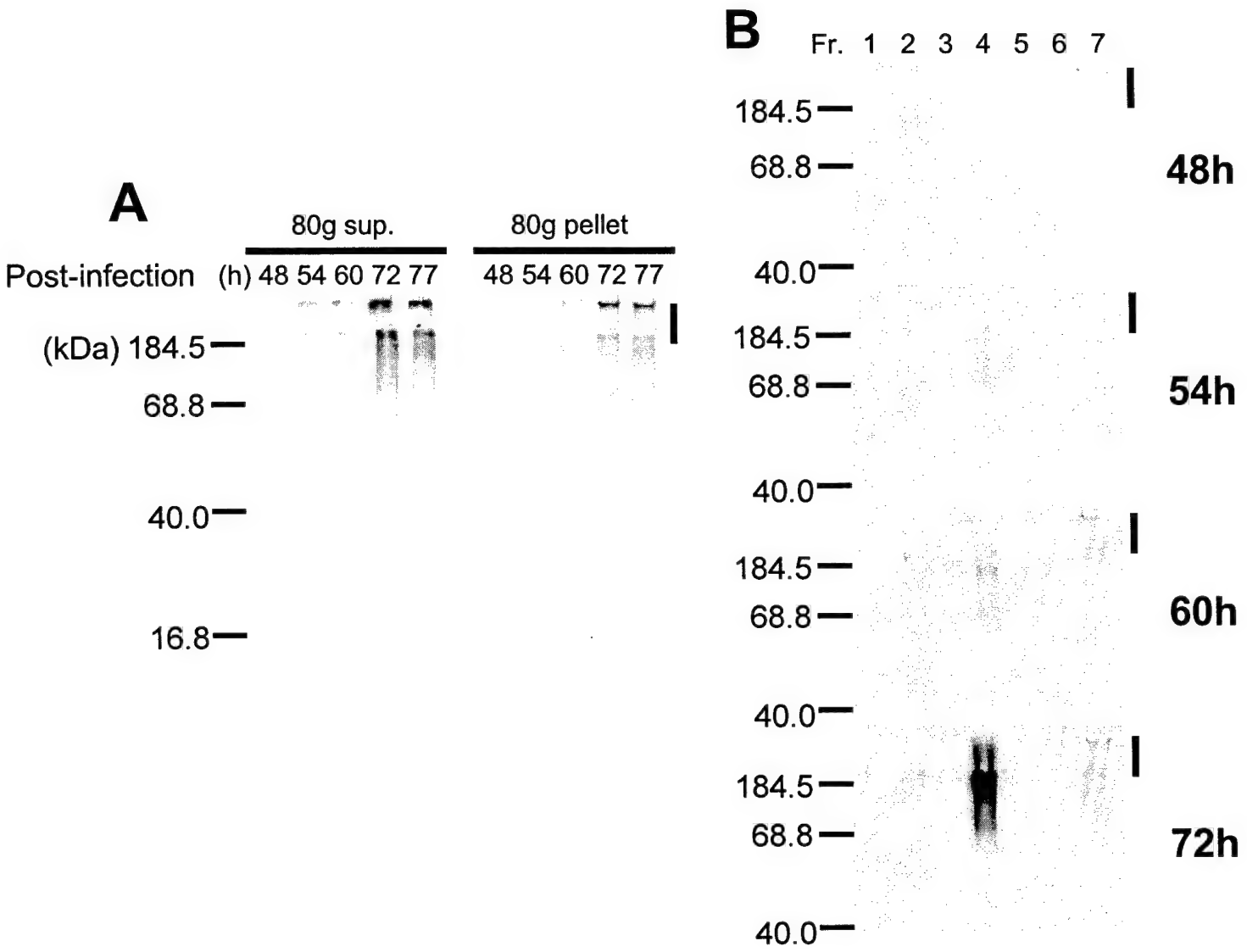
A
80g sup.
80g pellet
Post-infection (h) 48 54 60 72 77
48 54 60 72 77
(kDa) 184.5
68.8
40.0
16.8
B
Fr. 1 2 3 4 5 6 7
184.5
68.8
48h
40.0
184.5
68.8
54h
40.0
184.5
68.8
60h
40.0
184.5
68.8
72h
40.0

Fig 7. Lee

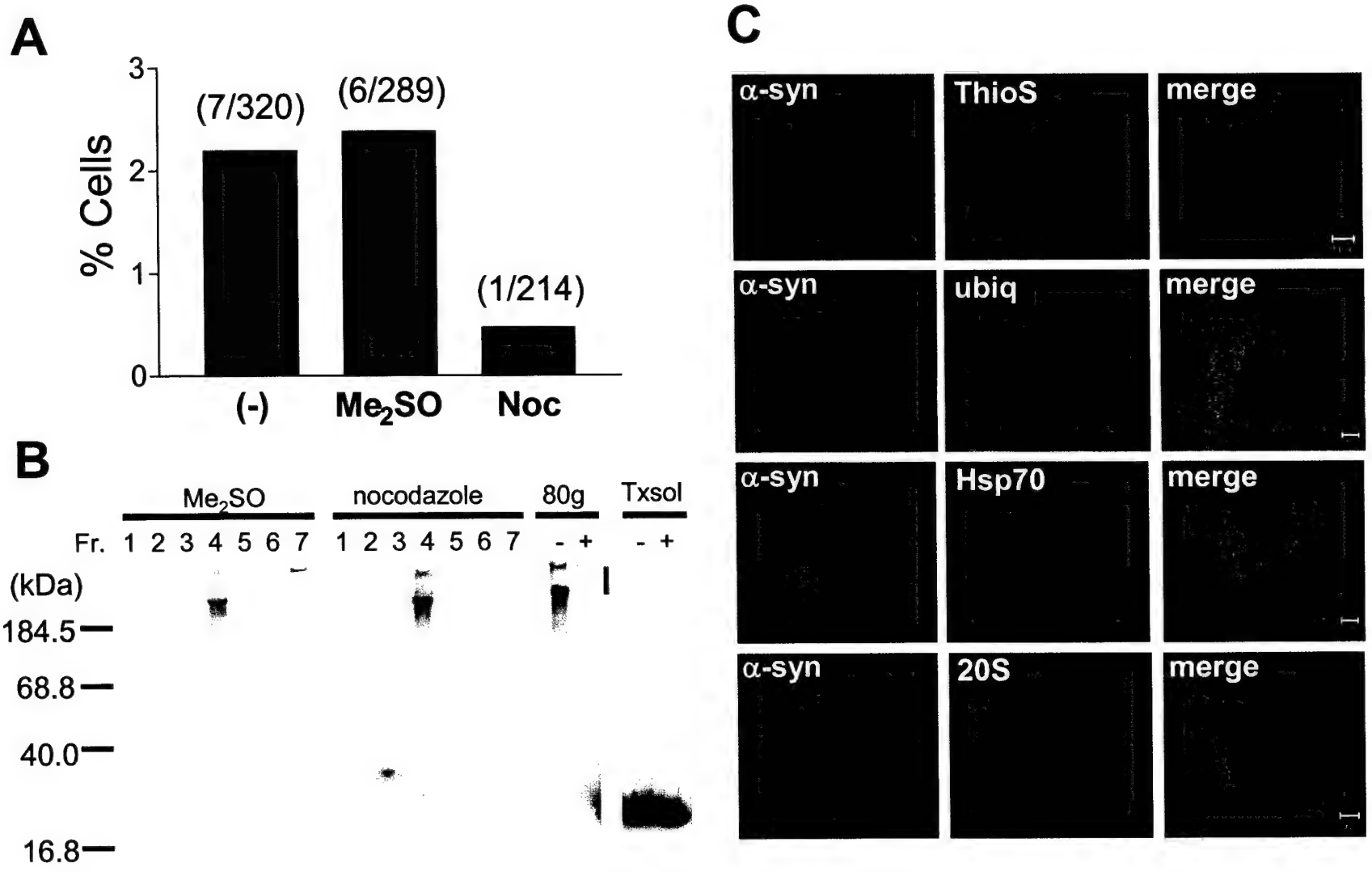
A
% Cells
3
2
1
0
(7/320)
(6/289)
(1/214)
(-)
Me2SO
Noc
B
Me2SO
nocodazole
80g
Txsol
Fr. 1 2 3 4 5 6 7 1 2 3 4 5 6 7 - + - +
(kDa)
184.5
68.8
40.0
16.8
C
α-syn
ThioS
merge
α-syn
ubiq
merge
α-syn
Hsp70
merge
α-syn
20S
merge

Appendix 2

Golgi Fragmentation Occurs in the Cells with Prefibrillar α-Synuclein Aggregates and Precedes the Formation of Fibrillar Inclusion

Nirmal Gosavi, He-Jin Lee, Jun Sung Lee*, Smita Patel, and Seung-Jae Lee

The Parkinson's Institute, Sunnyvale, California 94089, USA

* Present address: Division of Molecular and Life Science, Pohang University of Science and Technology, Pohang, Republic of Korea

Correspondence should be addressed to Seung-Jae Lee: The Parkinson's Institute, 1170 Morse Ave., Sunnyvale, CA 94089, Tel: 408-542-5642, Fax: 408-734-8522, Email: slee@thepi.org

Running title: Golgi fragmentation by prefibrillar α-synuclein aggregates

This work was supported by the U. S. Army Medical Research Acquisition Activity (DAMD17-02-0171) and the Abramson Family Foundation. J.S.L. was supported by a visiting fellowship from BK21 project, Ministry of Education, Republic of Korea.

Summary

Amyloid-like fibrillar aggregates of intracellular proteins are common pathological features of human neurodegenerative diseases. However, the nature of pathogenic aggregates and the biological consequences of their formation remain elusive. Here, we describe (i) a model cellular system in which prefibrillar α-synuclein aggregates and fibrillar inclusions are naturally formed in the cytoplasm with distinctive kinetics, and (ii) a tight correlation between the presence of prefibrillar aggreagtes and the Golgi fragmentation. Consistent with the structural abnormality of Golgi apparatus, trafficking and maturation of dopamine transporter through the biosynthetic pathway are impaired in the presence of α-synuclein aggregates. Reduction in cell viability was also observed in the prefibrillar aggregate-forming condition and before the inclusion formation. The fibrillar inclusions, on the other hand, show no correlation with Golgi fragmentation and are preceded by these events. Furthermore, at the early stage of inclusion formation, active lysosomes and mitochondria are enriched in the juxtanuclear area and co-aggregate into a compact inclusion body, suggesting that the fibrillar inclusions might be the consequence of the cell's attempt to remove abnormal protein aggregates and damaged organelles. These results support the hypothesis that prefibrillar α-synuclein aggregates are the pathogenic species and suggest the Golgi fragmentation and subsequent trafficking impairment as the specific consequence of α-synuclein aggregation.

Introduction

Many human neurological disorders, including Parkinson's disease, dementia with Lewy bodies, and multiple system atrophy, are characterized by amyloid-like fibrillar aggregates of α-synuclein, such as Lewy bodies (LBs)[1] and Lewy neurites (1,2). α-Synuclein is a 140-amino acid protein that is enriched in presynaptic terminals of neurons (3). In the test tube, this protein forms fibrils, which resemble the ones isolated from postmortem brains with LB diseases (4-6). A causative role of fibrillar α-synuclein inclusions in neurodegeneration has been suggested in a mouse model in which formation of intracytoplasmic α-synuclein inclusions coincided with the severe motor impairment (7). On the other hand, a study in a transgenic fly model that express human α-synuclein, has shown that co-expression of molecular chaperone hsp70 alleviated the neurodegenerative phenotype, but did not reduce the formation of α-synuclein-positive inclusion bodies (8). This result raised a question as to whether the fibrillar inclusions play a causative role in neurodegenerative process. Furthermore, recent *in vitro* studies revealed various non-fibrillar species during the course of fibrillation and suggested a possibility that these metastable intermediate species, not the fibrils themselves, might elicit cytotoxicity (9,10). Elucidating which particular aggregate species possesses the principal cytotoxic effect holds the key to understanding the etiologic role of protein aggregation in the disease pathogenesis. Study of this problem, however, has been hampered by the lack of experimental system in which intermediates of the endogenous fibrillation process can be biochemically defined and analyzed. Here, we have

established such a system and have assessed the effects of prefibrillar intermediates that are formed naturally in the cytoplasm. In this report, we refer to prefibrillar aggregates as non-fibrillar oligomeric assemblies that precede the formation of fibrils, and inclusions as large deposits of aggregates that are usually found in juxtanuclear location.

Materials and Methods

Antibodies

Monoclonal anti-α-synuclein antibody, LB509, was purchased from Zymed Laboratories (South San Francisco, CA), and a polyclonal anti-α-synuclein serum, 7071, was provided by Peter Lansbury (Brigham and Women's Hospital, Boston, MA). Antibodies against GM130, TGN46, and calnexin were obtained from BD Biosciences (San Diego, CA), Serotec (Oxford, UK), and StressGen Biotechnologies Corp. (Victoria, BC, Canada), respectively. Antibodies for mannosidase II and DAT were purchased from Chemicon (Temecula, CA). All the fluorescently labeled secondary antibodies were purchased from Jackson ImmunoResearch Laboratories (West Grove, PA). ^{125}I-labeled anti-mouse IgG antibody was obtained from Amersham Biosciences (Piscataway, NJ). Goat anti-mouse IgG antibody that is conjugated with 10 nm gold particle was obtained from Ted Pella Inc. (Redding, CA).

Aggregation analysis at different multiplicity of infection (MOI)

Different amounts (see Fig. 1 legend) of adeno/α-syn (11) and empty viral vector were mixed to make the final number of viral particle be 1.5×10^8. COS-7 cells (1.5×10^6 cells) were infected with these mixtures as described previously (11). At day 3, the cells were extracted in phosphate-buffered saline (PBS) with 1% Triton X-100 and protease inhibitor cocktail (Sigma), and the extracts were centrifuged at 16,000g for 5 min to separate detergent-soluble (supernatant) and insoluble (pellet) fractions. The pellets were

resuspended in half the volume of 1 x Laemmli sample buffer. Ten μg of supernatant and the equal volume of pellet were applied onto 12% SDS-polyacrylamide gel and subjected to Western blotting (12). For the quantitative analysis, the proteins were visualized using ^{125}I-labeled secondary antibody, and the monomers and the aggregate smears (from 60 kDa to the top of the gel) were quantified by computer-assisted densitometry using ImageQuant software (Molecular Dynamics) under equal light and power settings. Three independent experiments were performed.

For the Golgi analysis and cell viability assay, the cells were split onto cover-glasses in 12-well plate and into 35-mm dishes, respectively, at day 1 (the next day of infection) and incubated until the time of analysis, usually day 3 or day 4. We have noticed that the time-course of the aggregation process changes slightly depending on the surface area of the tissue culture dish; i.e., aggregation is faster in 100-mm dishes than in 35-mm dishes. To normalize the effects of viral vector itself, total amount of viral particles were adjusted to be equivalent with empty viral vector in all experiments.

Extraction and separation of prefibrillar aggregates and fibrillar inclusions

COS-7 cells were infected with adeno/α-syn at the MOI of 75, and, the cells were split into 35-mm dishes at day 1 and incubated until day 3 or day 4. On the day of extraction, buffer T (0.25 M sucrose, 25 mM KCl, 5 mM $MgCl_2$, 20 mM Tris, pH 7.5, 1% Triton X-100, Protease inhibitor cocktail) was added gently onto each dish and incubated at room temperature for 5 min. The Triton X-soluble supernatant was removed carefully, and

then buffer N (0.1 M Na_2CO_3, pH 11.5 with 1% Triton X-100 and Protease inhibitor cocktail) was added to each dish, and extract was obtained by scraping dishes and repeated pipetting. After incubation on ice for 5 min, the extract was centrifuged at 80g for 5 min, at which condition only the fibrillar inclusions sedimented to form a pellet[2]. The prefibrillar aggregates in the supernatant were collected by additional centrifugation at 16,000g for 10 min.

Fluorescence microscopy

Fluorescence staining, including nuclear staining with Hoechst 33258, was performed according to the procedures in Lee *et al.* (11). For the staining of lysosomes and mitochondria, the cells were incubated with 100 nM Lysotracker (Molecular Probes) and 200 nM Mitotracker (Molecular Probes), respectively, in the growth medium for 30 min, and then fixed and permeabilized. Morphology of GA was visualized using an antibody against GM130, TGN46, or mannosidase II. All the fluorescence images in this study were obtained with a laser scanning confocal microscope (LSM PASCAL; Zeiss). For quantitative analysis, images were obtained by the "tile-scan" of area of 0.48 mm^2, and the number of cells with fragmented Golgi (Fig. 3) or fibrillar inclusions (Fig. 2) was counted in three random areas. Each image contained 140 cells on average, and the experiment was repeated more than three times. Golgi fragmentation was defined as the dispersion of small Golgi immunoreactive foci. Only the cells with completely scattered Golgi fragments were counted, while the cells with long tubular Golgi staining were not.

Thus, the percentage obtained in this study is likely to under-represent the actual degree of Golgi fragmentation.

Electron microscopy

For electron microscopy (EM), α-synuclein was expressed in COS-7 cells at the MOI of 75 for 4 days. The sections were prepared as described in Bouley *et al.* (13). Briefly, the cells were fixed in 2% glutaraldehyde in 0.1 M phosphate buffer, pH 7.2, on ice for 35 min. After the post-fix in 1% osmium tetroxide at room temperature for 30 min, the cells were stained with 1% uranyl acetate for 1 h and then dehydrated with a series of different concentrations of ethanol. After the samples were embedded in gelatin capsule, the sections were prepared on carbon-coated nickel grads and stained with 1% uranyl acetate. For the immunolabeling, the sections were incubated in 1% gelatin/PBS, followed by 0.03 M glycine/PBS. After a rinse with 2% bovine serum albumin (BSA)/PBS, the sections were incubated with LB509 antibody (1/250 dilution) in 2% BSA/PBS, and then with 10 nm gold-conjugated goat anti-mouse IgG antibody. The sections were then stained with 1% uranyl acetate and lead citrate and observed with Philips CM 12 electron microscope.

Biotinylation and isolation of cell surface proteins

Cells were infected with various ratio of α-synuclein and empty viral vectors as described before and incubated until day 3. For the expression of dopamine transporter (DAT), the infected cells were transfected with hDAT /pCDNA3.1(+) on the next day. Biotinylation

and isolation of cell surface proteins were carried out according to Melikian et al. (14), and all the procedures performed on ice except indicated otherwise. Briefly, the cells were rinsed twice with PBS^{2+} (PBS with 0.1 mM $CaCl_2$ and 1.0 mM $MgCl_2$) and incubated with 1.0 mg/ml NHS-SS-biotin (Pierce, Rockford, IL) in PBS^{2+} for 20 min twice. Remaining reactive NHS-SS-biotin was quenched with 0.1 M glycine for 20 min twice, and then the cells were extracted in RIPA buffer [10 mM Tris, pH 7.4, 150 mM NaCl, 1.0 mM EDTA, 0.1% SDS, 1% Triton X-100, 0.5% sodium deoxycholate, protease inhibitor cocktail (Sigma)]. The cell extracts with same amounts of protein were incubated with Immunopure streptavidin-bead (Pierce) at room temperature for 45 min with constant rotation. The bound fractions were washed four times with RIPA buffer and eluted with 1x Laemmli sample buffer. The unbound fractions were precipitated with 5% trichloroacetic acid and dissolved in 1x Laemmli sample buffer. The samples were loaded onto SDS-PAGE and analyzed by Western blotting. Due to the abundance of cytoplasmic DAT relative to the cell surface DAT, one-hundredth equivalents of unbound samples (cytoplasmic proteins) were loaded.

Cell viability assay

The cells were trypsinized, and one-tenth of cells were mixed with the equal volume of 0.4% trypan blue solution (Sigma). The number of cells that exclude the dye was counted using hemocytometer in triplicate. Data in Fig. 10 was obtained from two independent experiments. The rest of the trypsinized cells were extracted and

fractionated as described above, and the detergent-insoluble fractions were subjected to Western blotting with LB509 antibody.

Results

Prefibrillar α-Synuclein Aggregates in the Cytoplasm

To characterize the aggregation process of α-synuclein in cells, we introduced various amounts of the cDNA into COS-7 cells using recombinant adenoviral vector (adeno/α-syn) and quantitatively analyzed the changes in the amounts of the monomers and aggregates. The level of monomers increased linearly with the increase of multiplicity of infection (MOI) before reaching a plateau (*ca.* 1.7% of total cellular protein). Once the monomer level reaches the plateau, the levels of aggregates elevated in response to increased MOI (Fig. 1A). This non-linear relationship between the monomer level and the aggregation allows us to selectively investigate the effects of the monomers or aggregates by choosing the appropriate MOI range. Two different types of α-synuclein aggregates were found by immunofluorescence staining: small punctate aggregates that are dispersed throughout the cytoplasm and large juxtanuclear inclusion bodies[2]. The large inclusions are strongly stained with thioflavin S, a fluorescent dye specific to amyloid-like structure, whereas the small punctate aggregates are not[2]. Electron microscopy (EM) shows that the inclusion bodies are filled with filaments with the width of 8-10 nm, and they are labeled with α-synuclein antibody (Fig. 1C). The presence of α-synuclein fibrils in the inclusions was further confirmed by immunogold labeling of individual fibrils that were isolated from the inclusion preparations[2]. Immuno-EM study also verified the non-fibrillar nature of small punctate aggregates upon isolation using the procedure described below[2].

Fig. 1

Small amount of aggregates appeared at day 2 post-infection and increased drastically at day 3 with a small further increase at day 4, while the monomer levels remained constant throughout this period (Fig. 2A). Until day 3, most of the aggregates were small, non-fibrillar ones, and less than 1% of cells had larger fibrillar inclusion bodies. However, during the 4th day, formation of fibrillar inclusion increased greatly (Fig. 2B). In order to confirm the time courses for the different aggregate species, we have recently established a biochemical method by which small non-fibrillar aggregates and fibrillar inclusions can be separated by their sizes and quantitated. After a series of extraction steps using detergent and basic pH, small non-fibrillar aggregates and fibrillar inclusions are separated into the supernatant and pellet, respectively, by a centrifugation at $80g^2$. When this procedure was applied to the time-course study, we found that small aggregates in the supernatant appeared at day 3 and sustained until day 4, whereas the inclusions in the pellet became apparent no sooner than day 4 (Fig. 2C), confirming that small non-fibrillar aggregates appear before the formation of fibrillar inclusions. Given the dye-binding property and the kinetic behavior, we propose that the small punctate aggregates are the cytoplasmic equivalents of prefibrillar intermediates of fibrillation.

Fig. 2

Golgi Fragmentation by Prefibrillar α-Synuclein Aggregates

To investigate cellular consequences specific to α-synuclein aggregation, we have examined the morphology of Golgi apparatus (GA) for two reasons: (i) α-synuclein aggregates may target membraneous organelles, as aggregates in our cell system appear initially in the membrane fraction[3], consistent with the earlier finding in cell-free assay that membrane-bound α-synuclein forms aggregates more efficiently than the cytosolic α-synuclein (15), (ii) fragmentation of GA has been found in several neurodegenerative diseases, including Alzheimer's disease (AD), amyotrophic lateral sclerosis (ALS), Creutzfeldt-Jakob disease (CJD), and multiple system atrophy (MSA) (16-18). Especially, the pathology of MSA is characterized by α-synuclein-positive inclusion bodies of neurons and oligodendrocytes (19-21). Thus, the morphological integrity of GA was analyzed with respect to the α-synuclein aggregation states using an immunofluorescence microscopy with the antibody against a cis-Golgi-specific matrix protein GM130. In cells with diffuse α-synuclein staining, the GA has normal compact morphology near the nucleus (Fig. 3A). However, the cells with prefibrillar aggregates frequently show fragmentation and dispersion of the GA (Fig. 3B and C). To determine if Golgi fragmentation is aggregation-induced event, cells with fragmented Golgi were counted at different MOI (Fig. 3D). Despite the presence of a high-level of soluble α-synuclein, Golgi fragmentation at a MOI of 20 was not different from the basal level. On the other hand, the Golgi fragmentation was significantly increased when prefibrillar aggregates formed with stable monomer levels (MOI of 75) (Fig. 3D), suggesting that increase of α-synuclein aggregates, rather than the monomer, might be the cause of Golgi

fragmentation. To confirm the correlation between α-synuclein aggregation and Golgi fragmentation, an independent experiment was carried out to score the Golgi fragmentation in a population of cells that contained small punctate aggregates. Golgi fragmentation was found far more frequently in the population with the aggregates (88.9% at MOI 75 and 66.7% at MOI 20) than in general population (11.5% at MOI 75 and 4.3% at MOI 20) (Fig. 3E). In contrast, expression of green fluorescence protein to *ca*. 9.1% of total cellular protein did not cause dramatic changes in the Golgi morphology (data not shown), suggesting that Golgi fragmentation is not a general consequence of overproduction of soluble proteins.

Fig. 3

To determine the effects of α-synuclein aggregates on other Golgi compartments, we examine the morphologies of trans- and mid-Golgi using antibodies against TGN46, an integral component of trans-Golgi membrane, and mannosidase II, a mid-Golgi resident enzyme. Dual immunofluorescence staining shows that the aggregate-induced Golgi fragments contain both GM130 and TGN46. Furthermore, these proteins stayed segregated to the opposite poles in these fragments as were in the normal compact GA (Fig. 4A), indicating that the cis-trans polarity was maintained even after the fragmentation. When the Golgi fragments were co-stained for GM130 and mannosidase II, the segregation of these proteins was also evident within the single fragments (Fig. 4B). However, the segregation was not as obvious as the co-staining of GM130 and

TGN46, probably due to their relative distance between the compartments. These results suggest that α-synuclein aggregate-induced Golgi fragmentation occurs in the entire Golgi complex without obvious disturbance of the cis-trans polarity.

Fig. 4

Reduction in cell surface level of dopamine transporter

While passing through the Golgi stacks, secretory and membrane proteins undergo a series of covalent modifications, such as glycosylation and deglycosylation, and the fully mature proteins are sorted to their final destinations. In order to assess functional consequence of the aggregate-induced Golgi fragmentation, we measured the changes in the cell surface level of a plasma membrane protein dopamine transporter (DAT). The cells were infected with different amounts of adeno/α-syn, and then transfected with DAT expression plasmids next day. After two more days of incubation, the cell surface proteins were covalently labeled with biotin and separated from the cytoplasmic proteins (non-biotinylated) using streptavidin-resin. Western analysis of these fractions shows that cell surface level of DAT was reduced in the prefibrillar aggregate-producing condition (MOI 75), compared to the empty vector alone (MOI 0) (Fig. 5). However, increase of monomeric α-synuclein level did not result in any change in the cell surface expression of DAT (Fig. 5, see MOI 7.5 and 25). Reduction in cell surface DAT was accompanied by the molecular weight shift of cytoplasmic DAT from 90 – 100 kDA to 56 kDA (Fig. 5). The former corresponds to the endoglycosidase H (endoH)-resistant

mature protein, and the latter the endoH-sensitive biosynthetic intermediate (14). Because the endoH resistance is obtained in mid-Golgi compartment, this data implies that the newly synthesized proteins cannot reach to the mid-Golgi in an aggregate-producing condition. In contrast, accumulation of endoH-sensitive form indicates that the overall protein synthesis and the initial glycosylation may not be compromised in this condition. These results suggest that prefibrillar α-synuclein aggregates cause the impaired protein trafficking and maturation through the biosynthetic pathway, probably by disrupting Golgi transport.

Fig. 5

Consistent with the finding that the biosynthesis of endoH-sensitive form of DAT is not affected by α-synuclein aggregation, the gross morphology and distribution of endoplasmic reticulum (ER) seem to remain unchanged in the presence of α-synuclein aggregates. Normally, the ER shows a dispersed reticular pattern throughout the cytoplasm. This pattern was maintained regardless of the α-synuclein aggregation state or structural integrity of GA in the cytoplasm (Fig. 6), suggesting that the α-synuclein aggregates have little effect on the ER morphology.

Fig. 6

Inclusion bodies may be cell's response to the toxic protein aggregates.

In contrast to the prefibrillar aggregates, no clear association was found between the fibrillar inclusions and the Golgi fragmentation. First, increase in Golgi fragmentation occurs before the appearance of fibrillar inclusions (Fig. 2B and 3F). Secondly, the size of the cell population that contains fragmented GA does not increase during the fourth day when a sudden increase in the number of fibrillar inclusions takes place (Fig. 2B and 3F). Finally, fragmented GA was rarely observed in the cells with fibrillar inclusions. Instead, two types of GA morphology were associated with fibrillar inclusions: in most cases, Golgi components were confined and dispersed inside the fibrillar inclusions (Fig. 7A), and occasionally, some cells maintained the compact, although slightly distorted, morphology of GA that surrounded the juxtanuclear fibrillar inclusions (Fig. 7B). The distorted compact Golgi that is adjacent to inclusion has also been reported previously in a study using a GFP-250 (N-terminal 252 amino acids of p115) chimera protein (22). These two types of Golgi morphology might be explained by the difference in the rate of conversion of prefibrillar intermediates to fibrillar inclusions; fast sequestration of the prefibrillar aggregates into the inclusions before they damage the GA might lead to the distorted compact Golgi adjacent to the inclusion body. Alternatively, inclusions could be formed from two different prefibrillar species, only one of which is capable of Golgi fragmentation. In any case, the fact that Golgi fragmentation occurs before the formation of inclusions and that some cells maintain the compact Golgi structure despite the presence of inclusions suggests that the inclusions themselves may not be the direct cause of the morphological disruption of the GA. Rather, co-staining of the fibrillar inclusions with α-synuclein and Golgi marker suggests that the inclusions might be a consequence

of the cell's attempt to remove abnormal protein aggregates and impaired organelles from the cytoplasm.

Fig. 7

Consistent with this interpretation, intact lysosomes and mitochondria accumulated in the juxtanuclear region at what appears to be an early stage of inclusion formation (Fig. 8A and C) and are also present in the compact inclusions (Fig. 8B and D). Lysosomes and mitochondria, which normally tend to be dispersed in the cytoplasm, showed a rather localized pattern in the juxtanuclear region in the presence of the prefibrillar α-synuclein aggregates (Fig. 8A and C). These organelles showed no sign of fragmentation and appear to be functionally intact, since the fluorescent dyes used in this study selectively accumulate in cellular compartment with low internal pH (lysotracker) or with the membrane potential (mitotracker). EM study also showed the accumulation of fragmented Golgi (Fig. 9, box 1) and intact mitochondria in the juxtanuclear region (Fig. 9). In addition, autophagosomes and lysosomes can be found in this area at the early stage of inclusion formation (Fig. 9, box 2). Proteasomes and chaperone molecules were also accumulated near the nucleus in the cells with α-synuclein aggrgates[2]. It has been suggested that the juxtanuclear pericentriolar region serves as the main location in which both autophagic/lysosomal system and ubiquitin-proteasome system execute their degradation function to remove abnormal proteins and damaged organelles (23-25). Thus, the localization of functional lysosomes and mitochondria in the juxtanuclear

region may be the manifestation of cell's defense mechanisms against the protein aggregates. Together, these results suggest that the formation of α-synuclein aggregates trigger the action of cellular defense system, which is represented by the accumulation of these aggregates and impaired organelles in the juxtanuclear region along with the mitochondria, autophagosomes/lysosomes, and proteasomes.

Fig. 8 and 9

Cytotoxicity of Prefibrillar α-Synuclein Aggregates

A cytotoxic effect of α-synuclein has been reported in several mammalian cell systems (26-29). However, the nature of toxic species has not been determined. To assess the cytotoxic effect of α-synuclein aggregates, we measured cell viability as a function of the occurrence of the aggregates. Increase of monomer, without forming aggregates, did not affect the viability (MOI 0-20) (Fig. 1A and Fig. 10A, day 3). In contrast, cell viability was significantly reduced when aggregates formed without increasing the monomer level (Fig. 10A and B, day3). Tight correlation between reduction in cell viability and α-synuclein aggregation was also found in the time-course study. Aggregates were formed at slower rates at lower MOIs (MOIs 20 and 50), and when they became apparent on the fourth day, the viability was reduced correspondingly (Fig. 10A and B). Like the Golgi fragmentation, reduction in cell viability occurred before the appearance of the fibrillar inclusions (Fig. 10A, day 3 at the MOI of 70, and see also Fig. 2B and C), implicating that the cytotoxic effect might be conferred by the prefibrillar aggregates. These results

suggest that the cytotoxic effect of α-synuclein depends on its ability to form aggregates, especially the prefibrillar intermediates.

Fig. 10

Discussion

In this study, we report two biological effects of cytoplasmic α-synuclein aggregates; fragmentation of the GA and cell death. The fact that these effects correlate only with the formation of aggregates, and not with the monomer level suggests that occurrence of these effects depends on the formation of higher-order, quaternary structures. The prefibrillar intermediates seem to be responsible for these effects, because both the effects occur in the presence of small prefibrillar aggregates, and before the formation of fibrillar inclusions. We were able to distinguish specific effects of prefibrillar intermediates from those of monomers and fibrillar inclusions by taking advantage of following features of our experimental system. First, once the monomer level reaches a plateau, only aggregates increase in response to increasing amount of α-synuclein cDNA without changing the monomer level. This phenomenon provides effective means to distinguish the effects of aggregates from those of monomers. Secondly, the ability to define naturally occurring prefibrillar aggregates and fibrillar inclusions biochemically, allowed kinetic analysis of each species. This study showed that the aggregation process of α-synuclein in cells, similar to the findings in test tube, involves prefibrillar intermediates in the course of forming fibrillar inclusions[2]. More importantly, such a kinetic delay of the inclusion formation enabled us to distinguish the cytophysiologic effects of prefibrillar intermediates and fibrillar inclusions.

Earlier examinations of human brain tissues and animal models have shown that the Golgi fragmentation was associated with the neurodegenerative phenotypes. Fragmentation of the GA has been found in human neurodegenerative diseases, including AD, ALS, CJD, and MSA (16-18). Moreover, transgenic mice expressing ALS-linked mutant superoxide dismutase (SOD)-1 showed Golgi fragmentation in spinal cord motor neurons in early, preclinical stage, implicating the role of Golgi fragmentation in early stage of neurodegeneration (30). Our present study links this well-documented pathological feature of neurodegenerative diseases, the Golgi fragmentation, to the prefibrillar aggregate form of α-synuclein. Although our results imply the correlation between Golgi fragmentation and cell death, they are not sufficient to suggest the cause/effect relationship between these two. Nevertheless, given the importance of the GA in maturation and trafficking of essential proteins and lipids, we speculate that synaptic sites might be particularly vulnerable to Golgi dysfunction. It is, therefore, noteworthy that transgenic mice producing non-fibrillar α-synuclein aggregates in neurons suffer from presynaptic degeneration in nigrostriatal system (31).

Whether inclusion bodies are toxic entities or harmless by-products or even a part of protective mechanism has been one of the central issues in amyloid-associated disorders. Our present study shows that (i) Golgi fragmentation and cell death are observed before the formation of inclusion bodies in mixed cell populations and that (ii) α-synuclein aggregates are pulled into the "pre-inclusion" area in the juxtanuclear region along with cellular defense organelles, such as autophagic/lysosomal vesicles and mitochondria.

These results are consistent with the notion that inclusion bodies *per se* might not be directly harmful to cells, rather they are consequences of the efforts to remove abnormal protein aggregates and damaged organelles from the cytoplasm. In a recent study using a drosophila model in which exogenous expression of human α-synuclein induced Lewy body-like inclusions and dopaminergic neuronal loss, overproduction of a molecular chaperone hsp70 alleviated the neurodegenerative phenotype without reducing the number of inclusion bodies (8). This study also argues against the direct role of α-synuclein-positive inclusion body in degenerative process. Non-causal relationship of inclusion bodies and cell death has also been proposed in other protein aggregation systems. Degenerative phenotype and the formation of detectable inclusion bodies have been dissociated in cell and animal models that overexpressed expanded polyglutamine-containing proteins (32-36). In another study using a transgenic mouse model that expresses familial ALS-associated mutant SOD1, small detergent-insoluble protein complex occurs before the on-set of disease phenotype, whereas the inclusion bodies can be detected once the clinical symptom is evident (37). Therefore, regardless of the constituent protein, inclusion body itself does not seem to be directly responsible for the cell death. However, these results do not exclude the possibility that the "process" of inclusion body formation might damage the cells; here, we refer to the "process" as the cellular events related to the inclusion formation *after* the diffusion-limited peripheral aggregation. For example, sequestration and depletion of vital proteins and organelles, such as proteasomes, mitochondria, and lysosomes, from the cytoplasm, as seen in the early stage of α-synuclein inclusion formation, could make the cells vulnerable to any

secondary stresses. The sequestration, thus the reduced cellular activity, of ubiquitin-proteasome system has indeed been proposed to be a general consequence of protein aggregation that can lead to cell death (38).

Interfering with the microtubule-mediated transport could also lead to the Golgi fragmentation. For example, microtubule-disrupting agents, such as nocodazole, cause a redistribution of Golgi proteins to ER exit sites (39). Thus, the Golgi fragmentation observed in our study could be a secondary consequence of overloading the microtubule-dependent transport system with the aggregates or of halting the trafficking at the negative ends of microtubules due to the accumulation of α-synuclein aggregates, rather than the direct effect of the α-synuclein aggregates. We do not have conclusive evidence to support either of these possibilities, but the architecture of the fragmented Golgi indicates that more complex mechanism may underlie the α-synuclein aggregate-induced Golgi fragmentation than the interference of microtubule-dependent transport. In case of the aggregate-induced Golgi fragmentation, components of different Golgi compartments seem to stay together in the Golgi fragments with the intact cis-trans polarity. This finding disagrees with what was observed during the nocodazole-induced Golgi fragmentation, in which trans-Golgi proteins were scattered more rapidly than mid-Golgi proteins, suggesting the separation of Golgi subcompartments from each other prior to the scattering (40).

Unlike the small punctate aggregates, juxtanuclear inclusion bodies contain α-synuclein fibrils. No evidence has been obtained for the presence of fibrillar α-synuclein aggregates outside the juxtanuclear inclusions. These findings implicate that although the mechanism is not understood at present, the structural transition of prefibrillar intermediates into thermodynamically more stable fibrils occurs after they are transported and deposited in the inclusion-forming site[2]. Recent study showed that α-synuclein fibrils were far less efficient in disrupting bilayer membranes than protofibrils (41), suggesting an inert nature of fibrils. In other studies using recombinant proteins or synthetic peptides that are not implicated in any disease, fibrils were non-toxic when treated to cultured cells, whereas the same treatment with non-fibrillar aggregates, that precede formation of fibrils, resulted in cell death (42). Therefore, formation of fibrillar inclusion bodies might protect the cells from the cytotoxicity of aggregates, not only by removing the prefibrillar aggregates from the cytoplasm, but also by providing the right environment for converting them to inert fibrils.

In conclusion, the results presented in this paper suggest that pathogenic property of α-synuclein may not stem from its primary structure, but from its ability to form toxic aggregates, particularly the prefibrillar aggregates. Importantly, fibrillar inclusions may not be directly toxic, rather they may represent the outcome of cell's natural way to handle abnormal protein aggregates that are formed randomly throughout the cytoplasm. Thus, both preventing the formation of aggregates and accelerating the conversion of

prefibrillar intermediates to fibrillar inclusions might be logical strategies for intervening the pathogenic progress of LB diseases.

Acknowledgements

We thank D. Di Monte and A. Manning-Bog for helpful comments on the manuscript. We also thank P. T. Lansbury for 7071 antibody, H. Melikian for DAT expression plasmid, and N. Ghori for the technical assistance for the EM.

References

1. Hardy, J., and Gwinn-Hardy, K. (1998) *Science* **282,** 1075-9.
2. Trojanowski, J. Q., Goedert, M., Iwatsubo, T., and Lee, V. M.-Y. (1998) *Cell Death Differ* **5,** 832-7
3. Goedert, M. (2001) *Nat Rev Neurosci* **2,** 492-501.
4. Giasson, B. I., Uryu, K., Trojanowski, J. Q., and Lee, V. M. (1999) *J Biol Chem* **274,** 7619-22
5. Conway, K. A., Harper, J. D., and Lansbury, P. T., Jr. (2000) *Biochemistry* **39,** 2552-63
6. Serpell, L. C., Berriman, J., Jakes, R., Goedert, M., and Crowther, R. A. (2000) *Proc Natl Acad Sci U S A* **97,** 4897-902
7. Giasson, B. I., Duda, J. E., Quinn, S. M., Zhang, B., Trojanowski, J. Q., and Lee, V. M.-Y. (2002) *Neuron* **34,** 521-533
8. Auluck, P. K., Chan, H. Y., Trojanowski, J. Q., Lee, V. M.-Y., and Bonini, N. M. (2002) *Science* **295,** 865-8.
9. Conway, K. A., Lee, S.-J., Rochet, J. C., Ding, T. T., Williamson, R. E., and Lansbury, P. T., Jr. (2000) *Proc Natl Acad Sci U S A* **97,** 571-6
10. Conway, K. A., Rochet, J. C., Bieganski, R. M., and Lansbury, P. T., Jr. (2001) *Science* **294,** 1346-9.
11. Lee, H.-J., Shin, S. Y., Choi, C., Lee, Y. H., and Lee, S.-J. (2002) *J Biol Chem* **277,** 5411-7.

12. Lee, S.-J., Liyanage, U., Bickel, P. E., Xia, W., Lansbury, P. T., Jr., and Kosik, K. S. (1998) *Nat. Med.* **4,** 730-734

13. Bouley, D. M., Ghori, N., Mercer, K. L., Falkow, S., and Ramakrishnan, L. (2001) *Infect Immun* **69,** 7820-31.

14. Melikian, H. E., and Buckley, K. M. (1999) *J Neurosci* **19,** 7699-710.

15. Lee, H.-J., Choi, C., and Lee, S.-J. (2002) *J Biol Chem* **277,** 671-8.

16. Gonatas, N. K., Gonatas, J. O., and Stieber, A. (1998) *Histochem Cell Biol* **109,** 591-600.

17. Sakurai, A., Okamoto, K., Fujita, Y., Nakazato, Y., Wakabayashi, K., Takahashi, H., and Gonatas, N. K. (2000) *Acta Neuropathol (Berl)* **100,** 270-4.

18. Sakurai, A., Okamoto, K., Yaguchi, M., Fujita, Y., Mizuno, Y., Nakazato, Y., and Gonatas, N. K. (2002) *Acta Neuropathol (Berl)* **103,** 550-4.

19. Wakabayashi, K., Hayashi, S., Kakita, A., Yamada, M., Toyoshima, Y., Yoshimoto, M., and Takahashi, H. (1998) *Acta Neuropathol (Berl)* **96,** 445-52.

20. Spillantini, M. G., Crowther, R. A., Jakes, R., Cairns, N. J., Lantos, P. L., and Goedert, M. (1998) *Neurosci Lett* **251,** 205-8.

21. Dickson, D. W., Liu, W., Hardy, J., Farrer, M., Mehta, N., Uitti, R., Mark, M., Zimmerman, T., Golbe, L., Sage, J., Sima, A., D'Amato, C., Albin, R., Gilman, S., and Yen, S. H. (1999) *Am J Pathol* **155,** 1241-51.

22. Garcia-Mata, R., Bebok, Z., Sorscher, E. J., and Sztul, E. S. (1999) *J Cell Biol* **146,** 1239-54.

23. Garcia-Mata, R., Gao, Y. S., and Sztul, E. (2002) *Traffic* **3,** 388-396.

24. Kopito, R. R. (2000) *Trends Cell Biol* **10,** 524-30.

25. Wigley, W. C., Fabunmi, R. P., Lee, M. G., Marino, C. R., Muallem, S., DeMartino, G. N., and Thomas, P. J. (1999) *J Cell Biol* **145,** 481-90.

26. Ostrerova, N., Petrucelli, L., Farrer, M., Mehta, N., Choi, P., Hardy, J., and Wolozin, B. (1999) *J. Neurosci.* **19,** 5782-5791

27. Zhou, W., Schaack, J., Zawada, W. M., and Freed, C. R. (2002) *Brain Res* **926,** 42-50.

28. Iwata, A., Maruyama, M., Kanazawa, I., and Nukina, N. (2001) *J Biol Chem* **276,** 45320-9.

29. Saha, A. R., Ninkina, N. N., Hanger, D. P., Anderton, B. H., Davies, A. M., and Buchman, V. L. (2000) *Eur J Neurosci* **12,** 3073-7

30. Mourelatos, Z., Gonatas, N. K., Stieber, A., Gurney, M. E., and Dal Canto, M. C. (1996) *Proc Natl Acad Sci U S A* **93,** 5472-7.

31. Masliah, E., Rockenstein, E., Veinbergs, I., Mallory, M., Hashimoto, M., Takeda, A., Sagara, Y., Sisk, A., and Mucke, L. (2000) *Science* **287,** 1265-1269

32. Klement, I. A., Skinner, P. J., Kaytor, M. D., Yi, H., Hersch, S. M., Clark, H. B., Zoghbi, H. Y., and Orr, H. T. (1998) *Cell* **95,** 41-53

33. Saudou, F., Finkbeiner, S., Devys, D., and Greenberg, M. E. (1998) *Cell* **95,** 55-66

34. Cummings, C. J., Reinstein, E., Sun, Y., Antalffy, B., Jiang, Y., Ciechanover, A., Orr, H. T., Beaudet, A. L., and Zoghbi, H. Y. (1999) *Neuron* **24,** 879-92

35. Faber, P. W., Alter, J. R., MacDonald, M. E., and Hart, A. C. (1999) *Proc Natl Acad Sci U S A* **96,** 179-84

36. Kazemi-Esfarjani, P., and Benzer, S. (2000) *Science* **287,** 1837-40

37. Johnston, J. A., Dalton, M. J., Gurney, M. E., and Kopito, R. R. (2000) *Proc Natl Acad Sci U S A* **97,** 12571-6.

38. Bence, N. F., Sampat, R. M., and Kopito, R. R. (2001) *Science* **292,** 1552-5.

39. Thyberg, J., and Moskalewski, S. (1999) *Exp Cell Res* **246,** 263-79.

40. Yang, W., and Storrie, B. (1998) *Mol Biol Cell* **9,** 191-207.

41. Volles, M. J., Lee, S.-J., Rochet, J. C., Shtilerman, M. D., Ding, T. T., Kessler, J. C., and Lansbury, P. T., Jr. (2001) *Biochemistry* **40,** 7812-9.

42. Bucciantini, M., Giannoni, E., Chiti, F., Baroni, F., Formigli, L., Zurdo, J., Taddei, N., Ramponi, G., Dobson, C. M., and Stefani, M. (2002) *Nature* **416,** 507-11.

Footnotes

[1] The abbreviations used are: LB, Lewy body; PBS, phosphate-buffered saline; MOI, multiplicity of infection; EM, electron microscopy; BSA, bovine serum albumin; GA, Golgi apparatus; AD, Alzheimer's disease; ALS, amyotrophic lateral sclerosis; CJD, Creutzfeldt-Jakob disease; MSA, multiple system atrophy; DAT, dopamine transporter; endoH, endoglycosidase H; ER, endoplasmic reticulum

[2] H.-J. Lee and S.-J. Lee, manuscript submitted

[3] J. S. Lee and S.-J. Lee, unpublished data

Figure Legends

Figure 1. **Non-linear relationship between the production of monomeric α-synuclein and its aggregation.** (A) COS-7 cells were infected with different amount of adenoviral vector (adeno/α-syn) carrying α-synuclein cDNA and incubated for three days, and the levels of monomers and aggregates were measured from detergent-soluble and insoluble fractions, respectively. Empty viral vector was added so as to make the total number of viral particles in each sample constant. Arbitrary optical density units are plotted in the graphs. Insets are the representative autoradiograms of the Western blotting using LB509 antibody and ^{125}I-labeled secondary antibody. Specific MOIs used in the Western analysis are: lane 1, 0; lane 2, 1; lane 3, 2.4; lane 4, 5; lane 5, 7.4; lane 6, 10; lane 7, 20; lane 8, 30; lane 9, 50; lane 10, 75; lane 11, 100. The vertical line on the right side of the inset indicates the stacking gel portion. (B) Juxtanuclear inclusion contains fibrils that are labeled with LB509 antibody. The image on the right side is the high-magnification view of the boxed region in the left image. Arrows indicate immunogold particles. No immunogold labeling was found in α-synuclein non-expressers. Scale bars, 1 μm (left image) and 0.1 μm (right image). N, nucleus; V, vacuole; I, juxtanuclear inclusion body

Figure 2. **Appearance of small non-fibrillar aggregates precedes the formation of fibrillar inclusions in cells.** (A) Time-dependent changes in the levels of monomers and aggregates at the MOI of 75 were measured from detergent-soluble (lower panel) and insoluble (upper panel) fractions, respectively. The vertical line on the right side

indicates the stacking gel portion. (B) The percentages of cells that contain juxtanuclear inclusion bodies were calculated at the indicated time points. α-Synuclein was expressed at MOI of 75. Images were obtained from two optical sections to ensure the detection of inclusion bodies that are located in a different plane. (C) Fibrillar inclusions (lane P) and prefibrillar aggregates (lane S) were separated based on their sizes at day 3 and day 4, and analyzed by Western blotting. The left and right panels show the detergent-insoluble aggregates and soluble monomers, respectively. The vertical line indicates the stacking gel portion.

Figure 3. **Occurrence of small α-synuclein aggregates is tightly associated with Golgi fragmentation.** Golgi morphology was visualized using an antibody against GM130. α-Synuclein was expressed at the MOI of 75, and α-synuclein aggregation (red) and Golgi morphology (green) were analyzed at day 3. Nuclei were stained with Hoechst 33258 (blue). (A) Diffuse α-synuclein staining and normal Golgi morphology. (B, C) Prefibrillar aggregates (arrowheads) that are dispersed throughout the cytoplasm and fragmented Golgi. Aggregates shown in (C) are larger than the ones in (B). Both types are non-fibrillar and associated with the Golgi fragmentation. (D) Percentage of cells with fragmented Golgi. α-Synuclein was expressed at given MOIs, and the cells were labeled with the antibodies against α-synuclein [7071 (5)] and GM130 at day 3. Total number of viral particles was adjusted to be equivalent by adding appropriate amount of empty viral vector to each sample. (E) In a separate experiment, number of cells with Golgi fragmentation was counted in a total cell population (total) and in a group of cells

with prefibrillar α-synuclein aggregates (Agg.) at day 3. Numbers above the bars represent the number of cells with fragmented Golgi per the number of cells counted. (F) Time-course of the Golgi fragmentation was analyzed at the MOI of 75 as described in (D). Scale bars, 10 μm

Figure 4. **α-Synuclein aggregates induce the Golgi fragmentation in the entire Golgi complex.** Aggregates were induced as in Fig. 3, and the cis- and trans-Golgi (A), or cis- and mid-compartments (B) were stained with the antibodies against GM130 (red) and TGN46 (green) (A), or GM130 (green) and mannosidase II (red) (B), respectively. The lower images in (A) are the high magnification views of normal (1) and fragmented Golgi (2). Note that the Golgi fragments contain all the markers that represent individual cisternae and still maintain the cis/trans polarity. Scale bars, 10 μm

Figure 5. **Reduction in cell surface expression of DAT and accumulation of biosynthetic intermediates in cytoplasm.** After the expression of α-synuclein at different MOIs for 3 days, cell surface levels of DAT were measured as described in Materials and Methods. Note that the cell surface level of DAT was reduced only in the condition that makes α-synuclein aggregates. Also note that α-synuclein monomer levels are similar at MOIs 25 and 75 (see Fig. 1). The bracket and the arrow indicate mature DAT and endoH-sensitive intermediate, respectively. Reduction in cell surface DAT is associated with the accumulation of biosynthetic intermediates in cytoplasm. Total amounts of viral particles were normalized with empty vector.

Figure 6. **No gross changes in ER morphology and distribution.** α-Synuclein was expressed at MOI 75 for 3 days. (A) Co-staining of α-synuclein (red) and ER (green). ER was stained with anti-calnexin antibody. A cell with aggregates is indicated with an arrow. No changes in ER morphology can be recognized in the presence of aggregates, compared to the cells with diffuse α-synuclein staining. (B) Co-staining of calnexin (red) and GM130 (green). The cells with fragmented GA are marked with arrows. ER morphology and distribution seem unchanged regardless of the state of GA. Scale bars, 10 μm

Figure 7. **GA in the cells with inclusion bodies.** α-Synuclein was expressed at MOI 75 for 4 days. (A) A fibrillar inclusion (arrow) containing GM130 (green). GM130 is dispersed within the inclusion body. The inclusion body shown here is present on a different optical plane from the majority of other cellular components. This type of inclusion is much more frequently found than the type shown in (B). (B) Distorted GA adjacent to a fibrillar inclusion (arrow). Scale bars, 10 μm

Figure 8. **Accumulation of lysosomes and mitochondria at the inclusion-forming site in aggregate-containing cells.** α-Synuclein was expressed at MOI 75 for 4 days. Cells with prefibrillar aggregates are indicated with arrows. (A) Lysosomes with internally low pH were labeled with Lysotracker. Lysosomes and α-synuclein aggregates were found in the juxtanuclear area that appears to be a "pre-inclusion" state. (B) Lysotracker

also stains the juxtanuclear inclusion body (arrowhead). (C) Mitochondria with intact membrane potential were labeled with Mitotracker. Functional mitochondria and α-synuclein were accumulated in the juxtanuclear region. (D) Mitochondria are also accumulated within the inclusion body (arrowhead). Scale bars, 10 μm

Figure 9. **EM analysis of the "pre-inclusion" state.** The cells were infected with adeno/α-syn at MOI 75, incubated for 4 days, and processed for EM as described in Materials and Methods. Most inclusions have compact structure with clear boundary. Occasionally, we observe what appears to be an early stage of inclusion formation. In this "pre-inclusion" stage, mitochondria (M), autophagosome precursors (arrows, box2), lysosomes (arrowhead, box 2), and fragmented GA (fGA, box 1) are accumulated in the juxtanuclear region, and hardly detected outside this region. Neither the pre-inclusion stage nor the compact inclusion body could be found in the cells that were infected with empty viral vector. Scale bars; 5.6 μm for the main image and 0.5 μm for the box images

Figure 10. **Cytotoxic effect of α-synuclein is dependent on the aggregation and occurs before the formation of fibrillar inclusions.** (A and B) COS-7 cells were infected with adeno/α-syn at given MOIs (the total number of viral particles was normalized by adding appropriate amount of empty vector), and each sample was subjected to the trypan blue exclusion assay (A) and Western blotting with LB509 (B).

The percentage of live cell number was calculated, with the non-expressor at day 3 as being 100%. The Western blotting was performed with the detergent-insoluble fractions.

Fig. 1

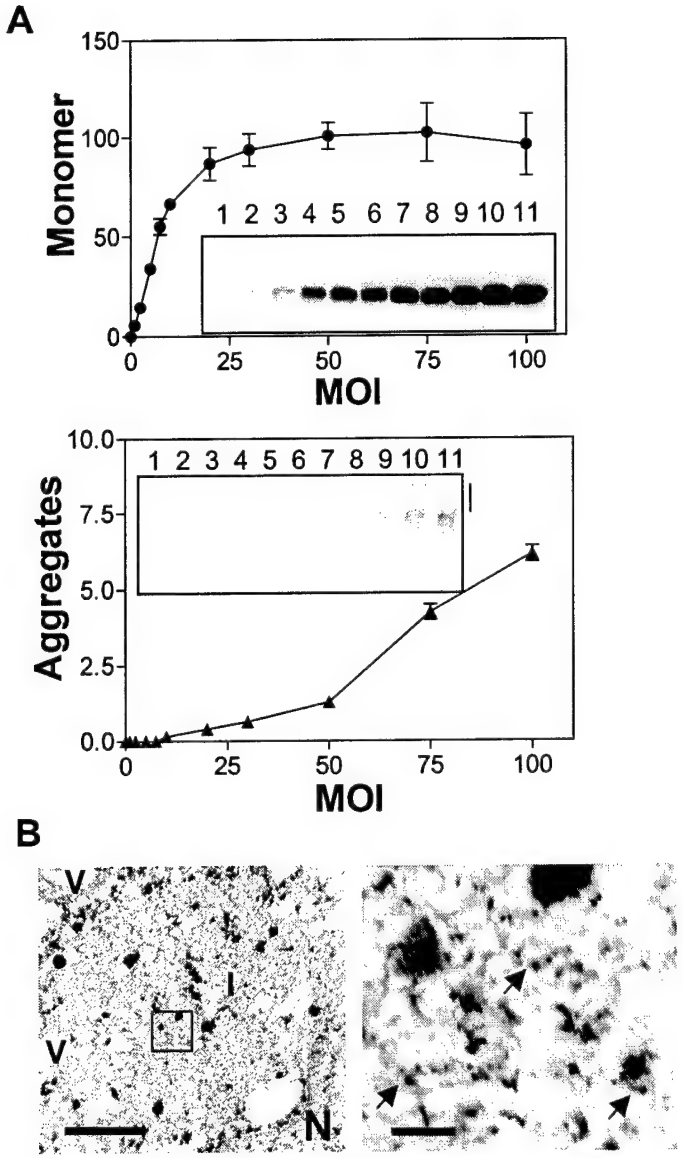
A
Monomer
150
100
50
0
1 2 3 4 5 6 7 8 9 10 11
0
25
50
75
100
MOI
Aggregates
10.0
7.5
5.0
2.5
0.0
1 2 3 4 5 6 7 8 9 10 11
0
25
50
75
100
MOI
B
V
I
V
N

Fig. 2

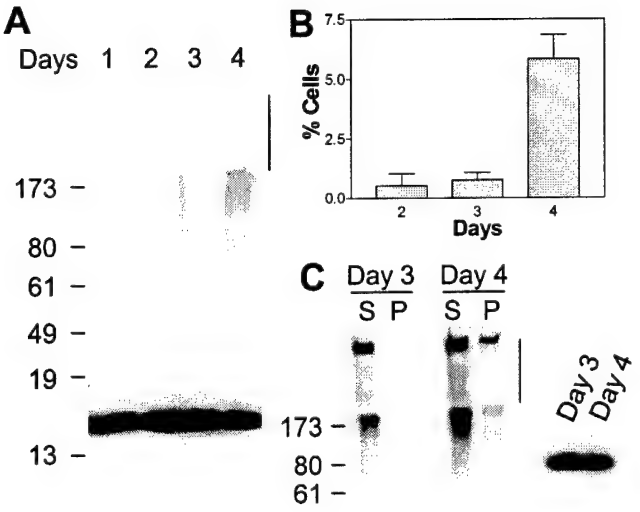
A
Days 1 2 3 4
173 –
80 –
61 –
49 –
19 –
13 –
B
% Cells
7.5
5.0
2.5
0.0
2
3
4
Days
C
Day 3
Day 4
S P
S P
173 –
80 –
61 –
Day 3
Day 4

Fig. 3

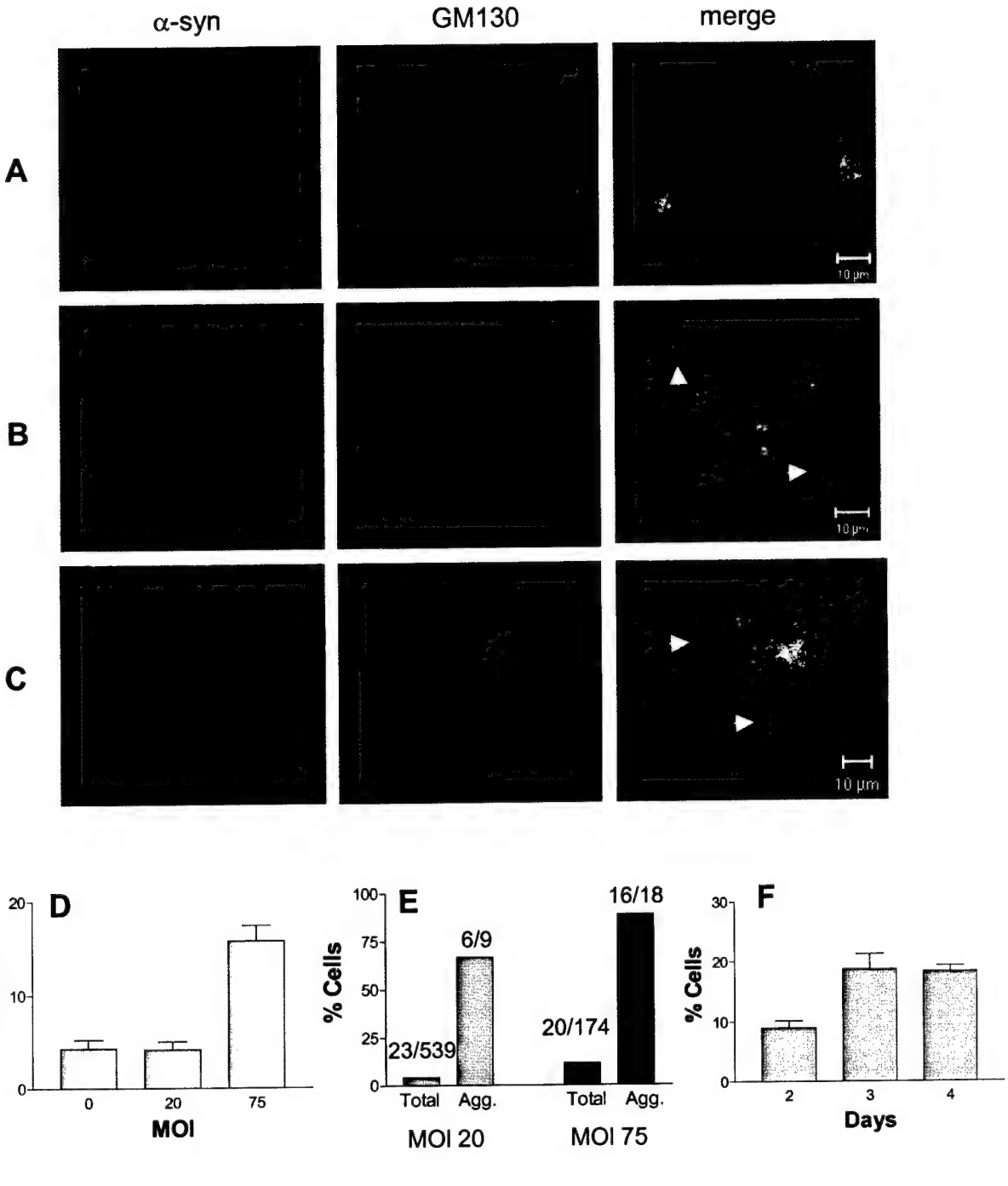
α-syn
GM130
merge
A
B
C
10 μm
10 μm
10 μm
D
% Cells
20
10
0
0
20
75
MOI
E
% Cells
100
75
50
25
0
23/539
6/9
20/174
16/18
Total
Agg.
Total
Agg.
MOI 20
MOI 75
F
% Cells
30
20
10
0
2
3
4
Days

Fig. 4

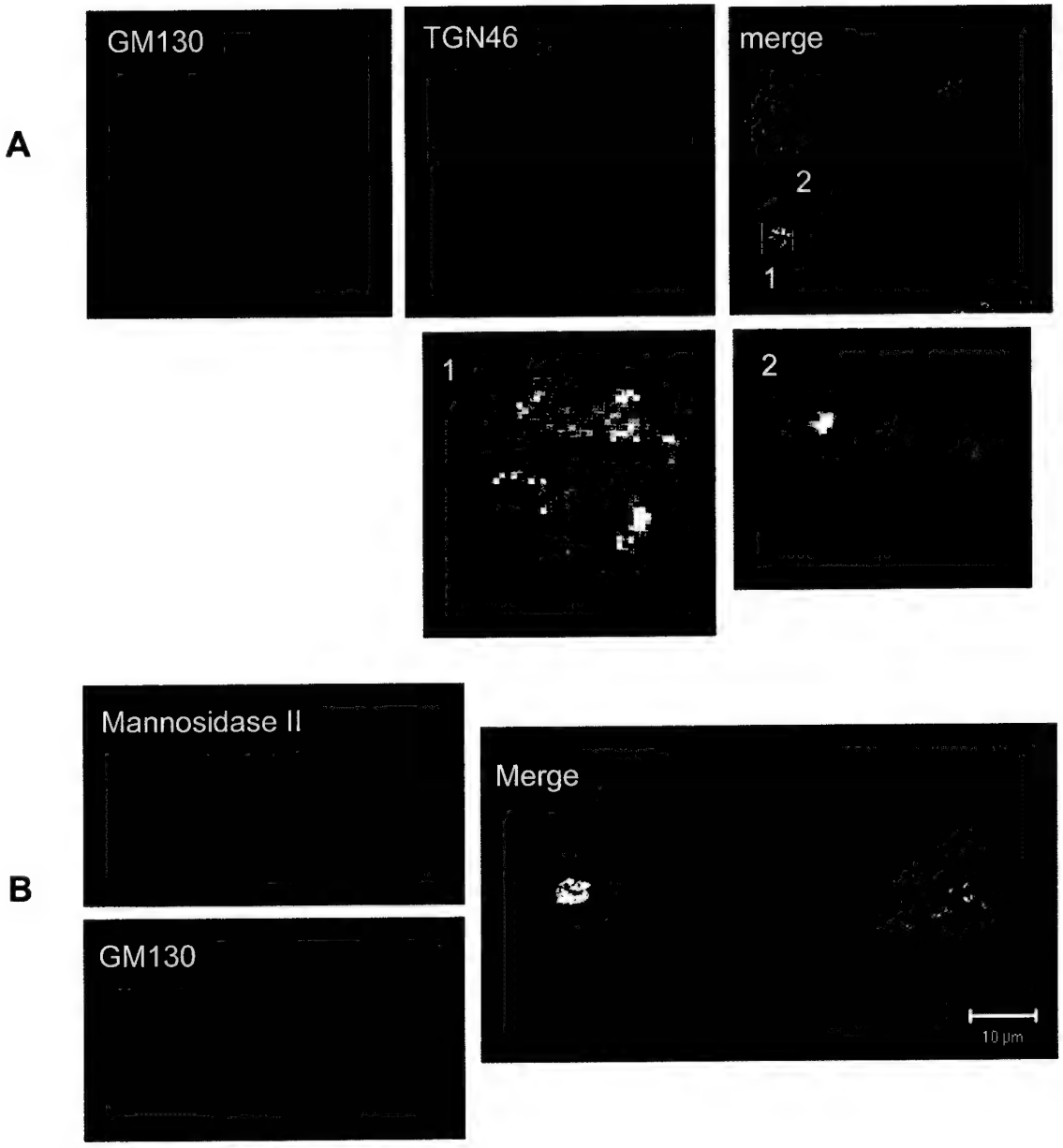

Fig. 5

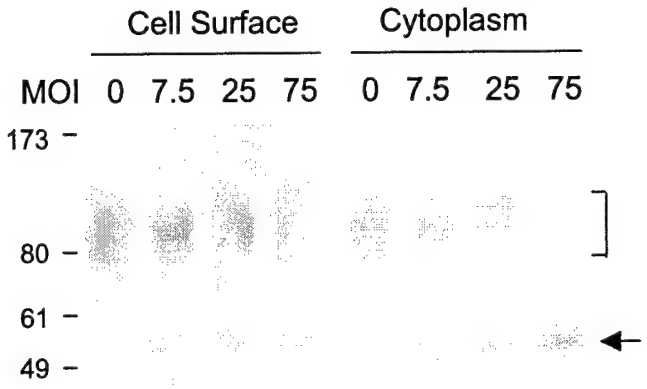

Fig. 6

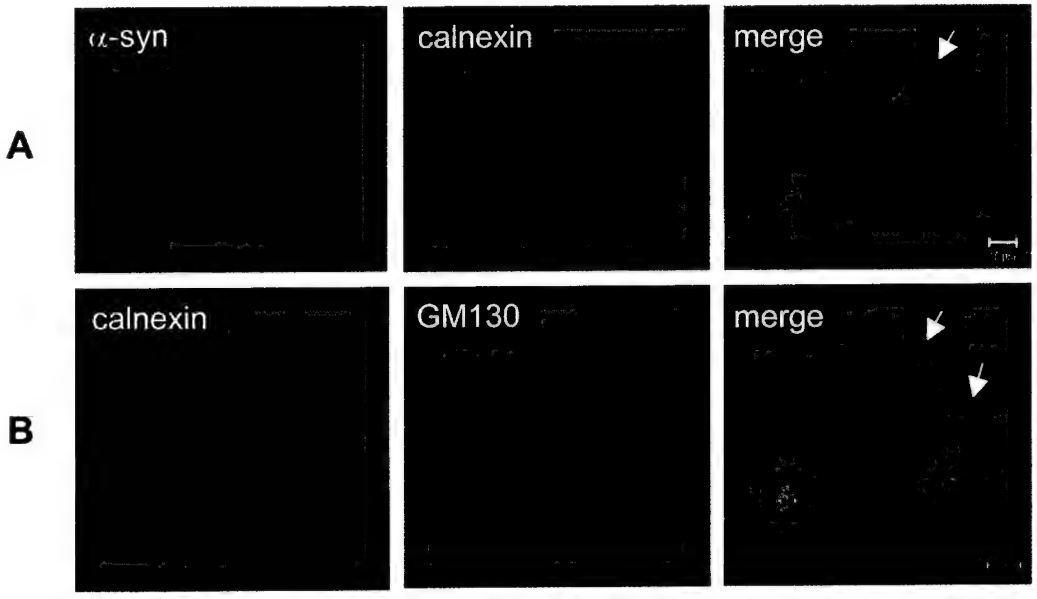

Fig. 7

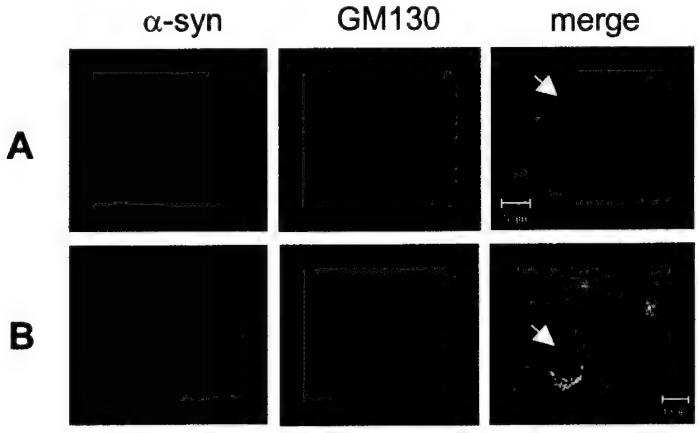

Fig. 8

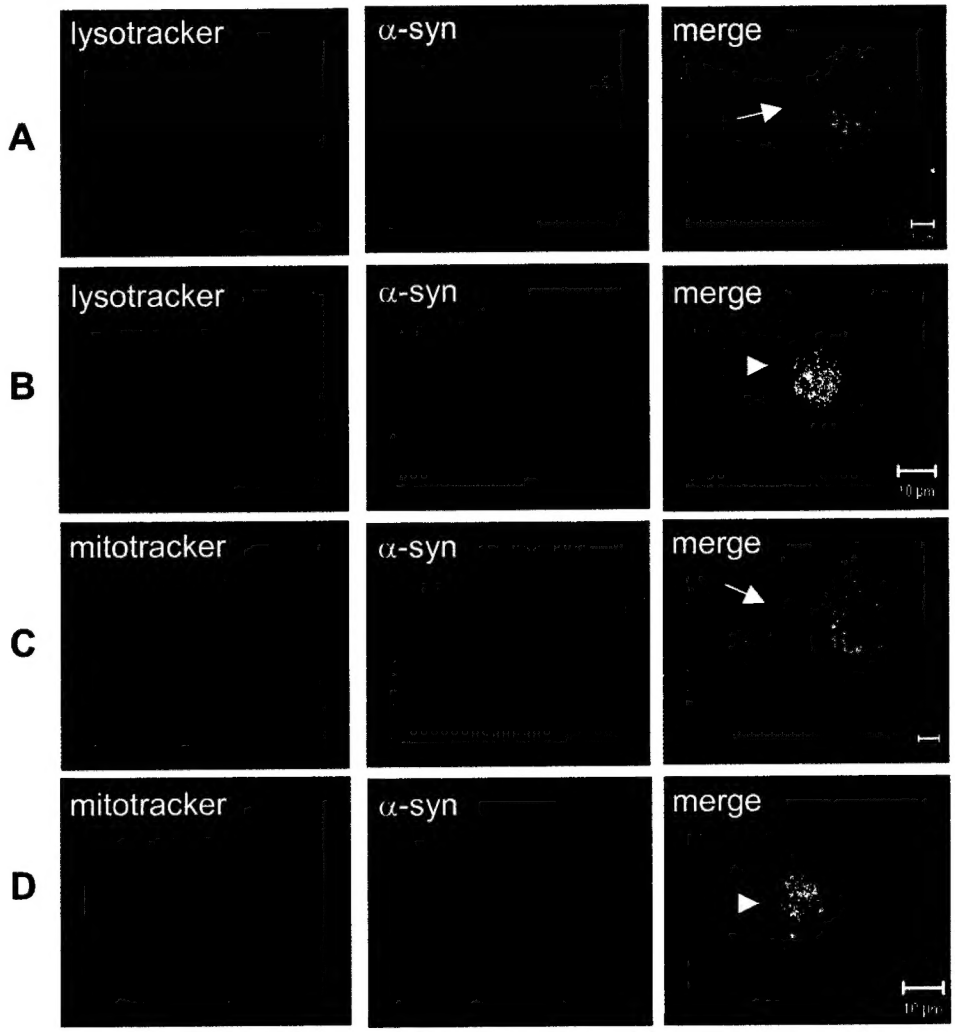
A
lysotracker
α-syn
merge
B
lysotracker
α-syn
merge
C
mitotracker
α-syn
merge
D
mitotracker
α-syn
merge

Fig. 9

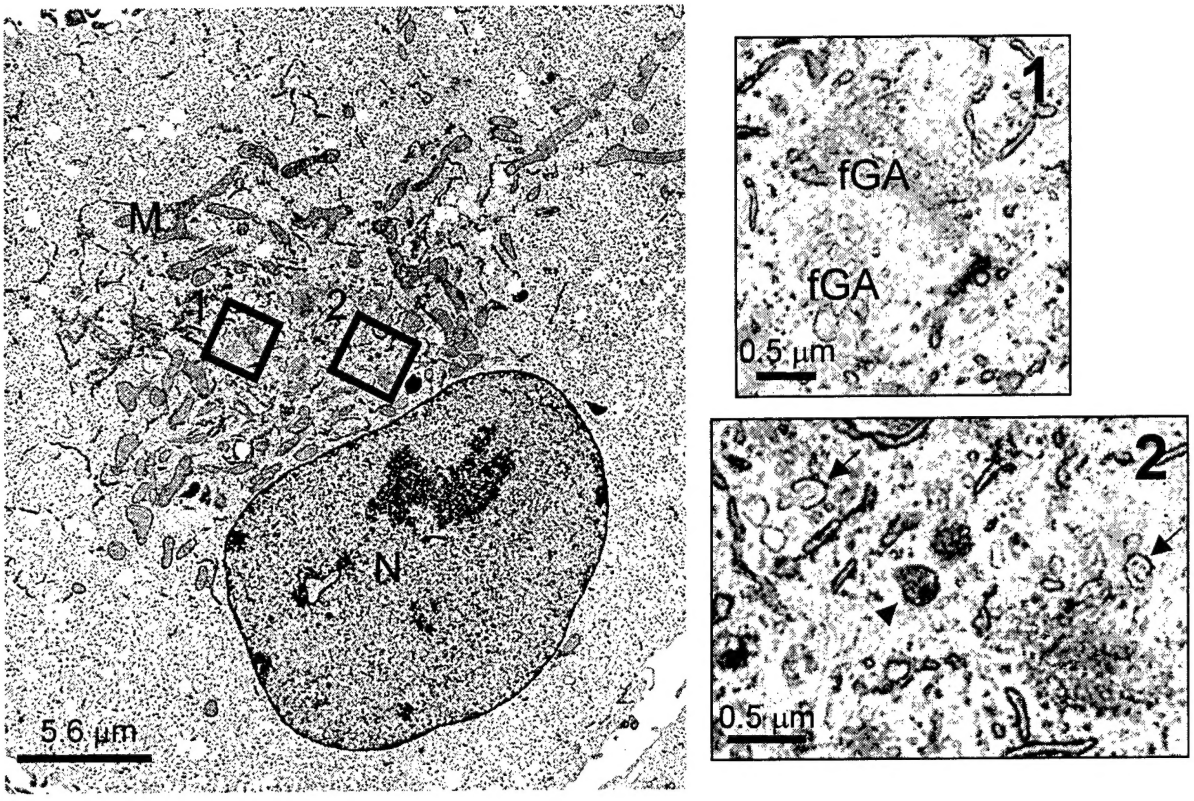

Fig. 10

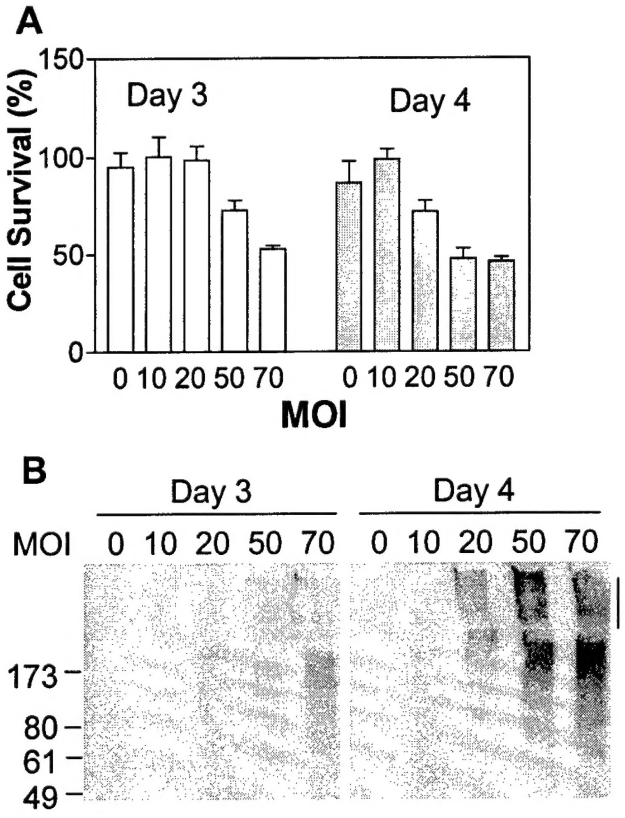
A
Cell Survival (%)
150
100
50
0
Day 3
Day 4
0 10 20 50 70
0 10 20 50 70
MOI
B
Day 3
Day 4
MOI
0 10 20 50 70
0 10 20 50 70
173
80
61
49

Appendix 3

D. Statement of Work

The overall goal of the proposed experiments is to elucidate the role of oligomeric α–synuclein in structural disassembly of membraneous organelles, especially the Golgi apparatus (GA). The rationale for this proposal stems from our recent study showing that prefibrillar oligomeric α–synuclein has ion channel activity in artificial liposomes and binds to brain microsomal membranes in an oligomerization-dependent manner. We intend to relate these novel oligomerization-dependent characteristics of α–synuclein to changes in morphological features of GA, which is linked to the cell death pathways.

1. In order to study the biological consequence of α-synuclein aggregation, we have recently established a cell culture model system, in which different aggregate species are formed with distinct kinetics. The first objective of the two-year project is to characterize the structural and compositional properties of the individual aggregate species. Especially, we will focus on identifying different subspecies of pre-fibrillar oligomeric aggregates. Following experiments will be carried out during the first year and a half.
   (i) We will develop a procedure by which different aggregate species can be separated by their size differences using a series of differential and gradient centrifugations.
   (ii) The structures of the isolated individual aggregates will be examined by electron microscopy and by a structure-sensitive fluorescent dye, thioflavin S, which is an indicator of amyloid-like fibrillar structure.
   (iii) Protein components of ubiquitin-proteasome system and molecular chaperones have been known to be present in the pathological α-synuclein aggregates in human brain. We will determine the presence of these proteins in each aggregate species using immunofluorescence techniques.
   (iv) Formation of each aggregate species will be analyzed by the fractionation and Western analysis at several different time points. This time-course analysis will provide insights into the precursor-product relationships between the different aggregate species.

2. In our cell system, we have found that the GA was fragmented when α-synuclein was overexpressed. The objective of this part of the project is to test the hypothesis that pre-fibrillar oligomeric form of α-synuclein, which has membrane-disrupting activity in a cell-free condition, is responsible for the Golgi fragmentation. Taking advantage of our cell system, in which the effects of monomer and different types of α-synuclein aggregates can be distinguished, we will examine the correlation between the Golgi fragmentation and the specific forms of α-synuclein. Immunofluorescent assessments of Golgi morphology and α-synuclein aggregation state will be performed both at single-cell level and in a population of cells. This experiment will start in the second half of the first year and will take about a year.

3. During the last six months of the project, we will test the hypothesis that pre-fibrillar oligomeric form is responsible for the α-synuclein-induced cell death. The ability to kinetically distinguish the different forms of α-synuclein aggregates in our cell system enables us to assess the cytotoxicity of these aggregates. The cytotoxicity will be analyzed using trypan blue exclusion assay and LDH assay. Also, the relationship between the Golgi fragmentation and cell death will be investigated by the fluorescent staining of dying cells with ethidium homodimer and immunofluorescent assessment of Golgi morphology.